IJSRM
INTERNATIONAL JOURNAL OF SCIENCE AND RESEARCH METHODOLOGY
An Official Publication of Human Journals

Human Journals
Research Article
August 2018 Vol.:10, Issue:2

Understanding the Potency of Heroin against Morphine and Cocaine

IJSRM
INTERNATIONAL JOURNAL OF SCIENCE AND RESEARCH METHODOLOGY
An Official Publication of Human Journals

Silvia Antonia Brandán*

Cátedra de Química General, Instituto de Química Inorgánica, Facultad de Bioquímica. Química y Farmacia, Universidad Nacional de Tucumán, Ayacucho 471, (4000) San Miguel de Tucumán, Tucumán, Argentina.

Submission: 22 July 2018
Accepted: 29 July 2018
Published: 30 August 2018

Keywords: Heroin, vibrational spectra, molecular structure, descriptor properties, DFT calculations.

ABSTRACT

Here, the structural, topological and vibrational properties of the free base, cationic and hydrochloride heroin species were theoretically determined in gas phase and in aqueous solution employing the hybrid B3LYP/6-31G* method. The results were compared with those reported for morphine and cocaine. The self-consistent reaction field (SCRF) and polarised continuum (PCM) methods were employed to study the solvent effects while the solvation energies were predicted with the solvation model. The N-CH_3 groups in the three species in both media were optimized in equatorial positions which apparently favour the volume expansions in solution, in particular, for cationic and hydrochloride species. The three heroin species presents the higher solvation energy values, as compared with the corresponding to morphine and cocaine. The charges studies and the molecular electrostatic potentials (MEP) mapped surfaces suggest clear electrophilic sites on the N-H group of the cationic species while the hydrochloride species shows nucleophilic regions around the Cl atoms but less weak sites on the C=O groups. The low bond order values for the Cl atoms in the hydrochloride species in both media reveal the ionic characteristics of their halogen H---Cl bonds. The NBO and AIM studies support the high stabilities of those three heroin species against to the corresponding to morphine and cocaine while the presence of other groups linked to tropane ring increase significantly the reactivity of alkaloid, specifically of its cationic and hydrochloride forms. The predicted higher global electrophilicity index (ω) for hydrochloride form of cocaine and the low global nucleophilicity index (E) values in heroin and morphine could probably explain the different behaviors of these species in both media. In this work, the known potential pharmacological properties for the three heroin species were explained easily with the rule of five states suggested by Lipinski's and Veber. The harmonic force fields and the complete vibrational assignments of the 144, 147 and 150 normal vibration modes expected respectively for the free base, cationic and hydrochloride heroin species were here reported for first time by using the SQMFF methodology and the available infrared and Raman spectra for the free base and hydrochloride forms.

INTRODUCTION

The tropane, cocaine, morphine and heroin alkaloids are known drugs with multiple biological properties for which are used in medicine for the treatment of severe pain [1-8] but its effects with the continual use, obviously change, generating addiction and dependence [1]. Consequently, when these drugs are used for non-medicinal purposes are named drugs of abuse and they are categorized as legal or illegal within the forensic science [5-9]. From this point of view, the detection of these alkaloids and its derivatives are generally performed by using a simple, quick and direct techniques such as the vibrational spectroscopy due to that in these cases the evidence clearly should be conserved [3,5,6,8,10-13]. Thus, both infrared and Raman spectra are tools highly suitable from long time to identify species in different aggregation states and where the Raman spectroscopy shows wide advantages against to the infrared in the case of a solid substance where is not necessary a previous sample preparation [3,5,6,8,10-13]. Besides, the identification of illicit drugs can be also studied with the Surface Enhanced Raman Spectroscopy (SERS) technique [14]. Obviously, the use of these spectroscopies are related to the structural studies because to perform the spectral analysis it is necessary to know the experimental structure and/or when it is unknown, the theoretical calculations are indispensable to predict the most stable structure [3,10-13]. Currently, the scaled quantum mechanical force field (SQMFF) methodology is a useful procedure enough used to perform the complete assignments of compounds combining the normal internal coordinates with the vibrational spectra and the corresponding harmonic force fields [15] and, for these reasons, that procedure is very reliable. With this methodology were recently obtained the scaled harmonic force fields for the base free, cationic and hydrochloride species of tropane, cocaine and morphine alkaloids by using transferable scaling factors and the Molvib program [16,17]. This way, the complete vibrational assignments for the three different forms of those three species were published and, now, these substances can be totally identified by using the vibrational spectroscopy [10-13]. In those works, the definitions of all normal internal coordinates of three species with fused cyclical structures constituted by different rings members and with a tertiary nitrogen atom were completely elucidated. But, so far, for the heroin alkaloid only the vibration normal modes for the base free were identified by using scaled frequencies with a scale factor of 0.96 above 800 cm^{-1} and by 1.0013 below 800 cm^{-1} while the other two cationic and hydrochloride species remain even without to assign [3]. Clearly, in that work the SQM methodology was not used and, for these reasons, the aims of this work are: (i) to known the most stable structures of base free,

cationic and hydrochloride species of heroin, (ii) to calculate some structural properties and, besides, (iii) to perform their complete vibrational assignments by combination of SQMFF approach with the corresponding normal internal coordinates and the experimental available infrared and Raman spectra for the base free and hydrochloride forms [18]. Structurally, heroin is an opiate derivative from morphine, therefore, heroin is known as diamorphine where two OH groups in the morphine structure were replaced by two acetyl groups forming heroin and, being it the most potent of the opiates [1]. The structures of heroin hydrochloride and its polymorph were already published by Canfield *et al.* [19] and Deschamps *et al.* [20], respectively. Then, to achieve those purposes these structures were used to perform the theoretical calculations based on the density functional theory (DFT) with the hybrid B3LYP/6-31G* method [21,22] and, after their optimizations, the structural properties and frequencies were calculated. Later, the complete vibrational assignments of the bands observed in the experimental available for the base free and the hydrochloride species were performed by using the normal internal coordinates, the corresponding scaled force fields computed with the SQMFF procedure and the Molvib program [15-17]. Finally, additional calculations on the frontier orbitals and some global descriptors were also computed [23-32] in order to know their reactivities and, also to understand the behaviours of those three species of heroin taking into account that the disease heroin crystal nephropathy is originated by heavy heroin abuse [33]. Here, the predicted properties including the solvation energies for the three species of heroin were compared with those reported for cocaine and morphine alkaloids [10-13].

Methodology calculations

The three species of heroin were modelled with the *GaussView* program [34] in accordance to the experimental structure reported for the hydrochloride form [19] and, later these species were optimized in gas phase with the Gaussian program Revision A.02 [35] by using the hybrid B3LYP/6-31G* method [21,22]. **Figure 1** shows the three structures of heroin together with the atoms labelling while **Figure 2** are presented the identifications of the five rings for each structure. On the other hand, the three species in solution were optimized at the same level of theory but with the self-consistent reaction field (SCRF) method and the integral equation formalism variant polarised continuum (IEFPCM) model [36,37] while the solvation model [38] was employed to calculate the solvation energies of the three species.

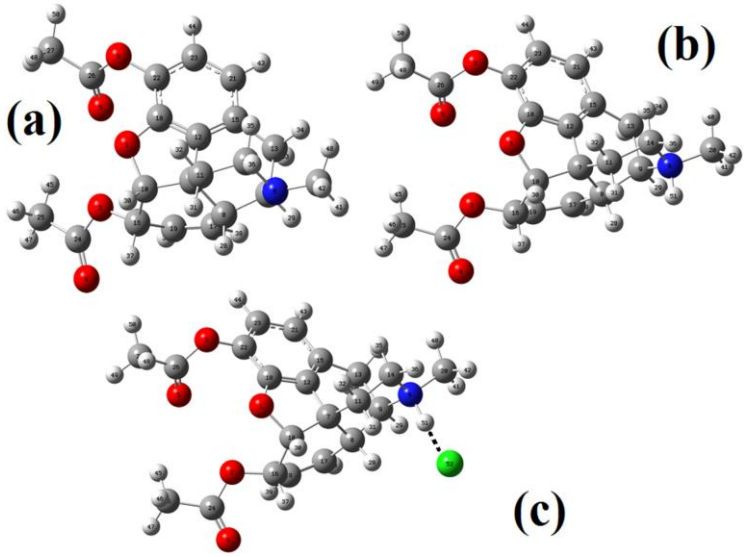

Figure 1. Theoretical molecular structures of the free base, cationic and hydrochloride species of heroin and the atoms numbering.

The Moldraw program [39] was used to calculate all volumes in both media while their corresponding variations were obtained as the differences between the values in solution and in gas phase at the same level of theory. The zero point vibrational energy (ZPVE) due to the electronic energy was employed to correct all energy values because the effects of molecular vibrations persist even at 0 K. Here, it is necessary to clarify that for the other alkaloids were also corrected the energy values. Then, with the optimized structures, the natural populations atomic (NPA) and the Merz-Kollman (MK) charges together with the molecular electrostatic potentials were calculated at the same level of theory [40,41] while the bond orders and the presence of donor-acceptor interactions were evaluated with the NBO program [40].

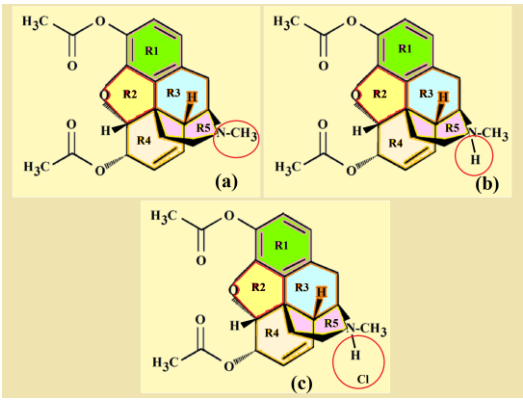

Figure 2. Theoretical simplified structures of the free base, cationic and hydrochloride species of heroin together with the identifications of their rings.

The AIM2000 program and the Bader's theory of atoms in molecules (AIM) were used to compute the topological properties of the three heroin species [42,43]. Here, the harmonic force fields by using the B3LYP/6-31G* level of theory were obtained for those three species by using the SQMFF methodology [15,16] with the Molvib program [17] while their normal internal coordinates were similar to those reported for the morphine species [11]. In addition, the assignments of all bands observed in the IR and Raman spectra for the free base and the hydrochloride species were performed by using potential energy distribution (PED) contributions ≥ 10%. The use of the frontier orbitals are of interest to explain the reactivities of heroin species [23,24] while their behaviours can be explained through global descriptors [11-13,25-32], such as the chemical potential (μ), electronegativity (χ), global hardness (η), global softness (S), global electrophilicity index (ω) and nucleophilicity indexes (E) descriptors [25-32]. The three heroin species were also estimated with some Lipinski's and Veber's criteria [44,45] in order to evaluate their pharmacological properties.

RESULTS AND DISCUSSION

Structural studies in gas phase and in solution

The results related to total energies, dipole moments, volume variations and solvation energies for the free base, cationic and hydrochloride species of heroin can easily be seen in **Table 1** compared with the values corresponding to the species of morphine and cocaine in both media [11,13]. The energy values for the three alkaloids and their species were corrected by ZPVE, as was explained in the above section. Note that the higher dipole moment values are observed for the cationic species, specifically in solution, as expected because these species are charged and, in solution, are highly hydrated with solvent molecules. The higher value is observed for the cationic species of heroin. On the other hand, the free base of heroin shows volume contraction while their cationic and hydrochloride species show volume expansions, as the hydrochloric species of morphine and the cationic species of cocaine. Here, the free base of cocaine presents similar volume expansion than its cationic form.

Figure 3 are presented the solvation energy and the dipole moment values for the different species of the three alkaloids in aqueous solution. Heroin presents the higher solvation energy values for the three species while the free base of heroin has higher solvation energy than cocaine and morphine but the hydrochloride cocaine species has lower value than the corresponding to heroin and morphine.

Table 1. Calculated total energies (*E*), dipole moments (μ), volume variations (ΔV) and solvation energies (ΔG) for the free base, cationic and hydrochloride heroin forms compared with those reported for the morphine and cocaine species in gas and aqueous solution phases.

B3LYP/6-31G*				
HEROIN[a]				
Gas phase corrected by ZPVE				
Species	E (Hartrees)	μ (D)	V (Å^3)	
Free base	-1244.5307	3.02	374.6	
Cation	-1244.9005	15.13	378.5	
H-Cl	-1705.3389	9.76	404.7	
PCM corrected by ZPVE				
	E (Hartrees)	μ (D)	V (Å^3)	ΔV (Å^3)
Free base	-1244.5534	4.65	374.1	-0.5
Cation	-1245.0073	21.50	380.1	1.6
H-Cl	-1705.3841	15.11	406.3	1.6
Solvation energy (kJ/mol)				
	$\Delta G_u^{\#}$	ΔG_{ne}	ΔG_c	
Free base	-59.54	29.13	-88.67	
Cation	-280.13	43.01	-323.14	
H-Cl	-118.56	43.38	-161.94	
MORPHINE[b]				
Gas phase corrected by ZPVE				
Species	E (Hartrees)	μ (D)	V (Å^3)	
Free base	-939.6185	2.77	292.7	
Cation	-939.9999	11.71	295.8	
H-Cl	-1400.4406	7.82	318.3	
PCM corrected by ZPVE				
	E (Hartrees)	μ (D)	V (Å^3)	ΔV (Å^3)
Free base	-939.6367	4.86	293.0	0.3
Cation	-940.1075	18.34	295.0	-0.8
H-Cl	-1400.4859	11.63	319.0	0.7
Solvation energy (kJ/mol)				
	$\Delta G_u^{\#}$	ΔG_{ne}	ΔG_c	
Free base	-47.74	13.17	-60.91	
Cation	-282.23	26.96	-309.19	
H-Cl	-118.82	25.92	-144.74	

COCAINE[c]				
Gas phase corrected by ZPVE				
Species	E (Hartrees)	μ (D)	V (Å^3)	
Free base	-1015.7564	1.55	321.0	
Cation	-1016.1483	9.57	322.5	
H-Cl	-1476.5594	7.45	353.2	
PCM corrected by ZPVE				
	E (Hartrees)	μ (D)	V (Å^3)	ΔV (Å^3)
Free base	-1015.7727	1.86	322.2	1.2
Cation	-1016.2309	13.22	323.7	1.2
H-Cl	-1476.5975	12.58	352.5	-0.7
Solvation energy (kJ/mol)				
	$\Delta G_u^{\#}$	ΔG_{ne}	ΔG_c	
Free base	-42.75	28.51	-71.26	
Cation	-216.66	38.58	-255.24	
H-Cl	-99.94	38.20	-138.14	

$\Delta G_u^{\#}$, See text; [a]This work; [b]From Ref [11]; [c]From Ref [13]

On the other side, from Fig. 3 it is observed that the graphic of dipole moment values shows clearly the higher values for the three species of heroin where the higher value observed for the cationic form justify evidently its higher solvation energy.

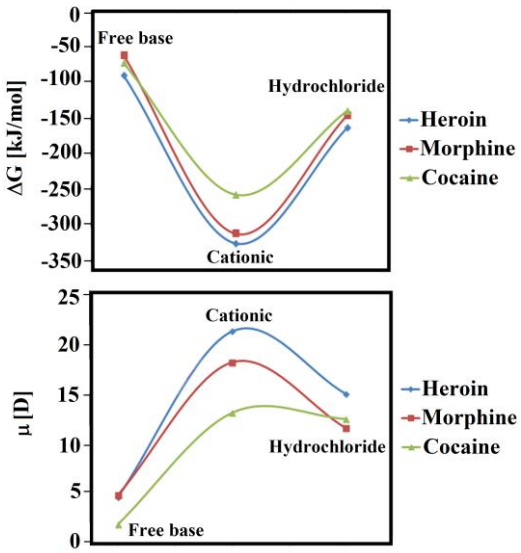

Figure 3. Solvation energies (upper) and dipole moment values (bottom) for the three forms of heroin compared with the corresponding to morphine and cocaine.

Here, the closers values of dipole moments observed for the hydrochloride species of morphine and cocaine probably support the similar solvation energy values observed in these two species. On the contrary, the proximities between the dipole moment values observed for the free base of heroin and morphine cannot be justified by the differences in their solvation energy values but, probably, the contraction and expansion volume observed for the free base of heroin and morphine, respectively could justify the differences in their corresponding solvation energy values.

All optimized geometrical parameters for the three heroin species in the two media by using the hybrid B3LYP/6-31G* method can be observed in **Table 2**. Calculated bond lengths are compared with those experimental ones determined by Canfield et al. [19] and Deschamps *et al.* [20] for diacetylmorphine and its polymorph form by using the root-mean-square deviation (RMSD). On the other side, bond angles were compared with those experimental values reported by Deschamps *et al.* [20] and with those theoretical calculated for the free base of heroin by Pandey *et al* [3] at the B3LYP/6-311G** level of theory while, the predicted dihedral angles were only compared with those two experimental values determined by Deschamps *et al.* [20] for the polymorphic form of heroin. Here, the better correlations in bond lengths were predicted for the three heroin species from the experimental data obtained by Deschamps *et al*. [20], with RMSD values between 0.029 and 0.020 Å while when the calculated values are compared with the experimental ones obtained by Canfield *et al.* [19] the RMSD values increase between 0.047 and 0.035 Å. In relation to the bond angles and for the two comparisons considered, the RMSD values show reasonable and practically similar concordances with values between 2.0 and 1.6 º. These results evidence, in particular for the free base, that with a basis set of lower size (6-31G*) similar bond angles values to those predicted by using 6-311G** basis set are obtained. Hence, these structures can be used to perform the corresponding vibrational analyses of the three species. Note that the dihedral angles show high RMSD values due to the great difference between the experimental and predicted dihedral C10-C16-O2-C24 angles. Besides, the hydrochloride species shows a strong change sign in the dihedral C22-O3-C26-C27 angle when the medium change of gas phase to aqueous solution.

Table 2. Comparison of calculated geometrical parameters for the free base, cationic and hydrochloride heroin species in gas and aqueous solution phases compared with the corresponding experimental ones for hydrochloride morphine.

Parameters	B3LYP/6-31G*[a]						Exp[b]	Exp[c]
	Free base		Cationic		Hydrochloride			
	Gas	PCM	Gas	PCM	Gas	PCM		
Bond lengths (Å)								
N6-CH_3	1.453	1.460	1.501	1.498	1.483	1.492		1.46
N6-C9	1.473	1.482	1.549	1.534	1.514	1.525		1.44
N6-C14	1.463	1.468	1.520	1.511	1.498	1.506		1.45
C8-C9	1.555	1.553	1.552	1.550	1.554	1.552		1.53
C9-C13	1.565	1.563	1.545	1.547	1.549	1.547		1.62
C7-C8	1.545	1.548	1.547	1.548	1.544	1.548		1.52
C7-C10	1.558	1.556	1.561	1.556	1.557	1.556		1.55
C7-C11	1.546	1.545	1.548	1.546	1.546	1.545		1.52
C7-C12	1.509	1.509	1.509	1.508	1.509	1.509		1.57
C12=C15	1.382	1.384	1.383	1.383	1.382	1.383		1.36
C8-C17	1.506	1.508	1.510	1.508	1.506	1.508		1.42
C10-C16	1.556	1.550	1.554	1.550	1.558	1.550	1.536(8)	1.55
C16-C19	1.510	1.509	1.511	1.509	1.510	1.509	1.480(8)	1.50
C12=C18	1.385	1.385	1.385	1.385	1.385	1.384		1.38
C17=C19	1.334	1.336	1.334	1.335	1.334	1.335		1.29
C16-O2	1.438	1.449	1.427	1.447	1.438	1.448	1.447(6)	1.45
C18-O1	1.364	1.372	1.362	1.371	1.363	1.371		1.37
C10-O1	1.461	1.472	1.455	1.470	1.463	1.470		1.48
C24-O2	1.354	1.350	1.368	1.351	1.357	1.351	1.338(8)	1.38
C24-O4	1.212	1.220	1.209	1.219	1.211	1.219	1.192(8)	1.23
C22-O3	1.395	1.403	1.382	1.401	1.392	1.402	1.403(7)	1.40
C26-O3	1.374	1.371	1.389	1.373	1.377	1.372	1.349(8)	1.31
C26-O5	1.204	1.214	1.202	1.213	1.204	1.214	1.180(9)	1.20
C24-C25	1.510	1.503	1.505	1.502	1.509	1.502	1.496(10)	1.45
RMSD[b]	**0.020**	**0.020**	**0.025**	**0.020**	**0.021**	**0.029**		
RMSD[c]	**0.035**	**0.035**	**0.047**	**0.043**	**0.040**	**0.041**		
Bond angles (º)								
Parameters	Gas	PCM	Gas	PCM	Gas	PCM	Exp[b]	Calc[d]
C9-N6-C20	114.2	112.9	114.3	114.1	114.5	113.9		114
C14-N6-C20	112.3	110.4	112.0	111.8	111.8	111.3		
C9-N6-C14	113.6	112.4	112.4	112.7	114.0	113.1		

N6-C9-C8	107.1	107.3	106.2	106.4	107.0	106.7		106
N6-C14-C11	111.1	111.6	110.5	110.9	110.9	111.2		111
C19-C16-C10	115.0	115.0	114.9	115.0	115.3	115.0	113.3(4)	115
C19-C16-O2	111.2	110.9	112.1	111.0	111.2	111.1	108.7(5)	107
C10-C16-O2	107.0	107.2	106.9	107.2	107.0	107.1	112.5(4)	111
C16-O2-C24	117.4	117.9	116.2	117.7	117.2	117.7	116.8(5)	
O2-C24-O4	124.0	123.5	122.6	123.4	123.7	123.3	123.6(6)	124
O2-C24-C25	109.9	111.1	110.2	111.0	110.1	111.0	112.2(6)	111
O4-C24-C25	125.9	125.3	127.0	125.4	126.0	125.5	124.1(6)	126
C18-C22-C23	117.8	118.1	117.5	118.0	117.8	118.1	117.4(6)	117
C18-C22-O3	121.8	122.4	122.4	122.5	121.8	122.3	123.4(6)	
C23-C22-O3	120.2	119.4	119.9	119.3	120.2	119.4	119.0(5)	122
C22-O3-C26	118.0	118.1	117.6	118.3	117.9	118.1	117.0(5)	
O3-C26-O5	124.0	122.9	122.8	122.8	123.7	122.8	121.6(6)	123
O3-C26-C27	109.5	110.6	109.6	110.5	109.6	110.5	112.4(7)	109
O5-C26-C27	126.3	126.4	127.4	126.5	126.6	126.5	125.9(7)	126
RMSD[b]	**1.7**	**1.6**	**1.8**	**1.6**	**1.7**	**1.7**		
RMSD[c]	**1.7**	**1.8**	**2.0**	**1.7**	**1.7**	**1.8**		
Dihedral angles (°)								
C8-C9-N6-CH_3	165.6	170.2	168.5	168.7	168.9	170.0		
C11-C14-N6-CH_3	-172.8	-176.8	-174.4	-175.5	-175.2	-176.7		
N6-C9-C8-C7	65.6	65.9	65.3	65.6	64.9	65.4		
N6-C14-C11-C7	-50.0	-50.7	-51.6	-50.3	-50.4	-49.9		
C19-C16-O2-C24	79.8	82.9	76.9	82.1	80.3	82.9		
C10-C16-O2-C24	-153.6	-150.6	-156.1	-151.4	-152.7	-150.5	-83.5(6)	
C16-O2-C24-O4	1.5	-0.3	0.7	-0.2	-0.1	-0.9		
C16-O2-C24-C25	-179.1	178.3	-179.5	178.5	179.0	177.8		
C18-C22-O3-C26	-72.0	-69.0	-68.3	-66.6	-73.4	-68.4	-94.2(8)	
C22-O3-C26-O5	-5.8	0.1	-3.7	179.4	-5.9	-0.3		
C22-O3-C26-C27	173.9	-179.3	176.5	179.4	174.0	-179.9		
O2-C16-C10-O1	-26.2	-30.7	-29.1	-31.2	-22.6	-30.6		
RMSD[b]	**52.0**	**50.7**	**54.5**	**51.8**	**51.1**	**50.8**		

[a]This work, [b]Ref [20] for free base heroin; [c]Ref [19] for free base heroin; [d]Ref [3] for free base heroin at the B3LYP/6-311G** level of theory. Bold letters: RMSD values.

Evidently, the Cl atoms have influence on its structure in solution and in the environmental, as expected due to its elevated electronegativity and, as supported by its volume expansion in solution (see Table 1). Figure 1 shows clearly that the cationic and hydrochloride species of heroin the N-CH_3 groups are optimized in equatorial position, in relation to N-H groups.

Evidently, these equatorial forms for these two species favor their volumes expansions in solution.

Charges, molecular electrostatic potential and bond orders (BO) analysis

Here, two atomic charges, molecular electrostatic potentials (MEP) and bond orders (BO) were studied for the three heroin species in order to analyze the differences between heroin and morphine because two acetyl groups are observed in the heroin species while each morphine species has only two OH groups. Hence, different properties are expected for those atoms belonging to R1 and R4 rings containing these groups in the three species. Thus, natural populations atomic (NPA), Merz-Kollman (MK) charges, molecular electrostatic potentials (MEP) and bond orders (BO) were calculated for the three heroin species by using the same level of theory in the two studied media [40,41]. Therefore, in **Table 3** are presented MK and MEP values for the three heroin species while in **Figure 4** can easily be observed the variations in the MK charges for the O, N and C atoms of those three species in both media. These graphics show clearly that the O atoms of those three species present practically the same behaviours in both media and, only slight variations in the MK charges are observed on the O1 and O2 atoms of hydrochloride species. However, the charges on N6 atoms in the free base in both media have negative signs while positive signs are observed on these atoms in the hydrochloride species in the two media. On the contrary, the MK charges on the N6 atoms in the cationic species in both media are practically nulls. In relation to the charges on the C atoms, it is observed that the charges on the C7, C8, C9 and C10 atoms, commons to the R1, R2 and R3 rings, in the free base present different signs in both media while, on C7 and C9 atoms are observed positive signs and, on C8 atoms negative signs. Here, very important results are observed in the charges on the C8 atoms for the cationic and hydrochloride species, respectively because the charges on those atoms increase notably in the hydrochloride species in solution while decrease in the cationic species in this media. On the contrary, the charges on the C9 atoms became negative and null, respectively in the hydrochloride and cationic species in solution, as observed in Fig. 4. Note that practically the same behaviours in the charges values are observed on the remaining C atoms but, in particular for the cationic species in solution, the charges on the C11, C12, C13 and C14 atoms became similar to the free base and hydrochloride species.

Table 3. Atomic MK charges and molecular electrostatic potentials for the most stable free base, cationic and hydrochloride structures of heroin by using the hybrid B3LYP/6-31G* level of theory.

Atoms	MK charges						MEP					
	Free base		Cationic		Hydrochloride		Free base		Cationic		Hydrochloride	
	Gas	PCM	Gas	PCM	Gas	PCM	Gas	PCM	Gas	PCM	Gas	PCM
1 O	-0.366	-0.370	-0.338	-0.363	-0,357	-0,330	-22,287	-22,290	-22,177	-22,179	-22,271	-22,269
2 O	-0.404	-0.412	-0.413	-0.404	-0,393	-0,382	-22,283	-22,283	-22,191	-22,190	-22,275	-22,273
3 O	-0.348	-0.374	-0.366	-0.368	-0,368	-0,388	-22,268	-22,268	-22,178	-22,177	-22,255	-22,252
4 O	-0.528	-0.539	-0.510	-0.520	-0,524	-0,528	-22,340	-22,344	-22,252	-22,259	-22,333	-22,335
5 O	-0.487	-0.503	-0.476	-0.493	-0,496	-0,499	-22,330	-22,335	-22,243	-22,250	-22,318	-22,320
6 N	-0.393	-0.373	0.016	-0.002	0,234	0,263	-18,354	-18,354	-18,062	-18,058	-18,248	-18,226
7 C	0.269	0.266	0.026	0.088	0,120	0,120	-14,715	-14,715	-14,579	-14,578	-14,695	-14,687
8 C	-0.134	-0.159	0.131	0.051	0,180	0,271	-14,726	-14,726	-14,573	-14,572	-14,705	-14,697
9 C	0.315	0.250	-0.048	0.008	0,012	-0,027	-14,700	-14,700	-14,519	-14,518	-14,656	-14,646
10 C	0.059	0.067	0.120	0.134	0,064	0,061	-14,672	-14,672	-14,555	-14,554	-14,657	-14,653
11 C	-0.332	-0.272	-0.181	-0.190	-0,126	-0,109	-14,735	-14,734	-14,582	-14,580	-14,712	-14,703
12 C	-0.388	-0.361	-0.304	-0.386	-0,371	-0,326	-14,750	-14,749	-14,629	-14,628	-14,730	-14,724
13 C	-0.282	-0.301	-0.156	-0.250	-0,281	-0,263	-14,731	-14,731	-14,580	-14,579	-14,696	-14,688
14 C	0.106	0.060	-0.034	0.004	-0,084	-0,085	-14,713	-14,713	-14,527	-14,524	-14,668	-14,656
15 C	0.323	0.317	0.218	0.288	0,290	0,266	-14,731	-14,731	-14,610	-14,608	-14,709	-14,703
16 C	0.436	0.469	0.372	0.406	0,388	0,317	-14,672	-14,672	-14,566	-14,564	-14,661	-14,658
17 C	-0.136	-0.135	-0.292	-0.262	-0,306	-0,337	-14,741	-14,741	-14,621	-14,619	-14,725	-14,721
18 C	0.439	0.415	0.384	0.442	0,397	0,309	-14,689	-14,689	-14,577	-14,575	-14,671	-14,666
19 C	-0.333	-0.336	-0.208	-0.230	-0,209	-0,190	-14,743	-14,742	-14,628	-14,625	-14,729	-14,725
20 C	-0.276	-0.296	-0.434	-0.443	-0,467	-0,472	-14,717	-14,717	-14,524	-14,522	-14,670	-14,661
21 C	-0.357	-0.353	-0.330	-0.348	-0,340	-0,333	-14,741	-14,741	-14,630	-14,628	-14,722	-14,717
22 C	0.042	0.081	0.126	0.099	0,107	0,184	-14,681	-14,680	-14,574	-14,572	-14,664	-14,659
23 C	-0.129	-0.152	-0.134	-0.122	-0,161	-0,186	-14,736	-14,735	-14,630	-14,628	-14,718	-14,713
24 C	0.720	0.720	0.722	0.711	0,722	0,727	-14,618	-14,619	-14,532	-14,534	-14,611	-14,610
25 C	-0.467	-0.434	-0.456	-0.438	-0,465	-0,469	-14,740	-14,739	-14,662	-14,665	-14,734	-14,731
26 C	0.748	0.774	0.749	0.768	0,770	0,768	-14,608	-14,610	-14,523	-14,526	-14,596	-14,595
27 C	-0.549	-0.550	-0.553	-0.561	-0,553	-0,549	-14,727	-14,727	-14,652	-14,654	-14,718	-14,716
28 H	0.068	0.080	0.027	0.040	0,031	0,008	-1,118	-1,118	-0,965	-0,964	-1,099	-1,093
29 H	0.033	0.059	0.102	0.101	0,084	0,094	-1,119	-1,120	-0,939	-0,938	-1,076	-1,067
30 H	0.062	0.056	0.075	0.069	0,077	0,081	-1,107	-1,107	-0,993	-0,991	-1,093	-1,089
31 H	0.088	0.075	0.060	0.056	0,053	0,051	-1,121	-1,121	-0,966	-0,965	-1,102	-1,092
32 H	0.109	0.094	0.136	0.133	0,092	0,088	-1,118	-1,118	-0,966	-0,964	-1,093	-1,084
33 H	0.075	0.087	0.123	0.140	0,118	0,117	-1,114	-1,113	-0,968	-0,966	-1,081	-1,073
34 H	0.096	0.105	0.074	0.093	0,088	0,084	-1,112	-1,111	-0,962	-0,960	-1,078	-1,069
35 H	0.023	0.034	0.104	0.099	0,062	0,060	-1,130	-1,129	-0,937	-0,934	-1,078	-1,065
36 H	0.078	0.086	0.105	0.096	0,111	0,115	-1,120	-1,120	-0,933	-0,931	-1,077	-1,065
37 H	0.005	-0.002	0.025	0.013	0,015	0,041	-1,107	-1,106	-1,001	-0,999	-1,097	-1,093
38 H	0.116	0.123	0.169	0.168	0,157	0,162	-1,108	-1,107	-0,987	-0,986	-1,092	-1,088
39 H	0.180	0.181	0.190	0.194	0,157	0,167	-1,110	-1,109	-1,001	-0,998	-1,098	-1,094
40 H	0.083	0.092	0.207	0.212	0,156	0,163	-1,124	-1,123	-0,924	-0,921	-1,067	-1,057
41 H	0.117	0.124	0.192	0.195	0,182	0,192	-1,116	-1,115	-0,923	-0,921	-1,068	-1,059
42 H	0.125	0.132	0.186	0.188	0,186	0,193	-1,118	-1,118	-0,923	-0,921	-1,071	-1,062

43 H	0.159	0.161	0.177	0.179	0,167	0,169	-1,109	-1,109	-1,000	-0,999	-1,090	-1,085
44 H	0.157	0.161	0.178	0.180	0,167	0,170	-1,103	-1,102	-1,003	-1,000	-1,087	-1,082
45 H	0.145	0.133	0.146	0.135	0,142	0,140	-1,112	-1,112	-1,031	-1,037	-1,106	-1,103
46 H	0.134	0.125	0.144	0.139	0,135	0,139	-1,101	-1,100	-1,023	-1,025	-1,095	-1,092
47 H	0.129	0.124	0.141	0.141	0,131	0,134	-1,113	-1,111	-1,036	-1,038	-1,107	-1,105
48 H	0.165	0.163	0.174	0.173	0,167	0,167	-1,092	-1,093	-1,017	-1,020	-1,082	-1,081
49 H	0.151	0.151	0.164	0.167	0,155	0,155	-1,103	-1,102	-1,028	-1,030	-1,093	-1,091
50 H	0.156	0.157	0.173	0.172	0,158	0,159	-1,095	-1,092	-1,019	-1,020	-1,085	-1,081
51 H			0.298	0.303	0,056	0,042			-0,808	-0,804	-0,988	-0,981
52 Cl					-0,630	-0,708					-64,506	-64,528

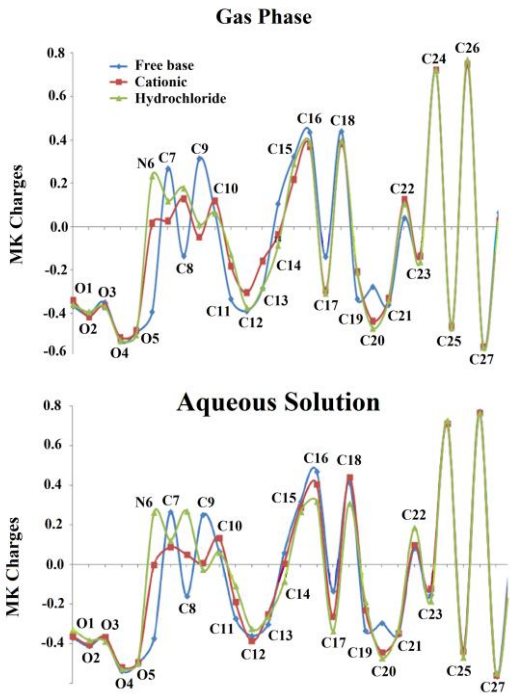

Figure 4. Variations of MK charges on the atoms from 1 to 27 for the three forms of heroin in the gas phase (upper) and in aqueous solution (bottom) compared with the corresponding to morphine and cocaine at B3LYP/6-31G level of theory.**

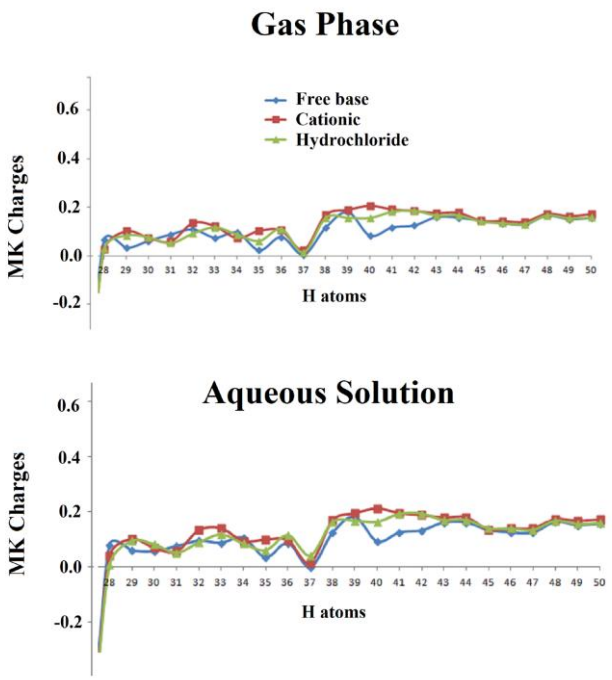

Figure 5. Variations of MK charges on the atoms from 28 to 50 for the three forms of heroin in the gas phase (upper) and in aqueous solution (bottom) compared with the corresponding to morphine and cocaine at B3LYP/6-31G level of theory.**

If now, the MK charges on the H atoms for the three species in both media are analysed from **Figure 5** similar behaviours are observed. However, the clear differences in the MK charges are observed on the H51 atoms of the cationic and hydrochloride species in both media observing the highest and lowest values on the atoms of the cationic and hydrochloride

species, respectively as expected because they are the less and most labile H atoms, especially in solution.

The NPA charges for the three heroin species in both media can be seen in **Table 4** together with the BO values. These NPA charges show practically the same behaviours in the three species in both media, observing only on the C16, C18, C22, C24 and C26 atoms positive signs while on the remaining C atoms and on the O and N atoms are observed negative signs. Obviously, on all H atoms are observed NPA charges with positive signs having the higher values the cationic species than the hydrochloride ones.

When the MEP values on all atoms of the three heroin species are analyzed the tendencies observed in these forms are in agreement with the higher electronegativities values of the involved atoms, hence, Cl > O > N > C > H, where the most negative values are observed on the Cl atoms of hydrochloride species while the less negative values are clearly observed on the H51 atoms of cationic and hydrochloride species in both media. Now, if the MEP mapped surfaces for the three species in gas phase are carefully evaluated by the different colorations from **Figure 6**, it is possible to observe for the free base strong red colours on both C=O groups belong to the acetyl groups and, besides a weak red colour on the N atom while weak blue colours are observed on H atoms that belong to C-H and N-CH_3 groups.

Table 4. NPA charges and Wiberg indexes for the most stable free base, cationic and hydrochloride structures of heroin by using the hybrid B3LYP/6-31G* level of theory.

Atoms	NPA charges						Wiberg indexes					
	Free base		Cationic		Hydrochloride		Free base		Cationic		Hydrochloride	
	Gas	PCM	Gas	PCM	Gas	PCM	Gas	PCM	Gas	PCM	Gas	PCM
1 O	-0.517	-0.517	-0.503	-0.501	-0.513	-0.511	2.114	2.112	2.131	2.128	2.120	2.120
2 O	-0.545	-0.541	-0.550	-0.543	-0.548	-0.545	2.156	2.162	2.138	2.150	2.151	2.155
3 O	-0.548	-0.548	-0.548	-0.544	-0.549	-0.548	2.153	2.153	2.149	2.155	2.152	2.153
4 O	-0.604	-0.610	-0.590	-0.599	-0.600	-0.602	2.026	2.016	2.043	2.028	2.031	2.024
5 O	-0.575	-0.576	-0.566	-0.574	-0.573	-0.573	2.060	2.053	2.072	2.056	2.064	2.056
6 N	-0.515	-0.510	-0.451	-0.448	-0.497	-0.484	3.119	3.111	3.472	3.472	3.353	3.387
7 C	-0.091	-0.090	-0.093	-0.092	-0.092	-0.091	4.004	4.004	4.005	4.004	4.004	4.004
8 C	-0.285	-0.286	-0.291	-0.292	-0.302	-0.305	3.942	3.942	3.943	3.943	3.920	3.920
9 C	-0.046	-0.049	-0.033	-0.036	-0.043	-0.041	3.927	3.928	3.851	3.853	3.884	3.876
10 C	0.107	0.107	0.108	0.106	0.108	0.108	3.849	3.850	3.849	3.850	3.843	3.845
11 C	-0.451	-0.452	-0.478	-0.476	-0.471	-0.473	3.899	3.898	3.879	3.879	3.877	3.877
12 C	-0.083	-0.082	-0.106	-0.104	-0.088	-0.088	3.987	3.987	3.982	3.982	3.987	3.987
13 C	-0.493	-0.494	-0.496	-0.495	-0.489	-0.492	3.892	3.891	3.875	3.875	3.886	3.884
14 C	-0.260	-0.263	-0.257	-0.258	-0.260	-0.259	3.867	3.868	3.779	3.780	3.816	3.810
15 C	-0.022	-0.021	-0.052	-0.049	-0.035	-0.036	3.994	3.994	3.992	3.993	3.994	3.994

16	C	0.033	0.034	0.027	0.027	0.030	0.030	3.845	3.844	3.856	3.854	3.844	3.843
17	C	-0.214	-0.213	-0.250	-0.247	-0.220	-0.221	3.950	3.949	3.937	3.937	3.948	3.946
18	C	0.310	0.311	0.316	0.316	0.314	0.315	3.916	3.917	3.916	3.918	3.917	3.918
19	C	-0.228	-0.227	-0.184	-0.184	-0.220	-0.215	3.949	3.948	3.938	3.938	3.947	3.947
20	C	-0.466	-0.469	-0.475	-0.473	-0.475	-0.473	3.815	3.816	3.714	3.713	3.753	3.743
21	C	-0.241	-0.242	-0.235	-0.235	-0.241	-0.241	3.945	3.945	3.940	3.940	3.944	3.944
22	C	0.246	0.246	0.272	0.270	0.253	0.255	3.902	3.901	3.916	3.915	3.906	3.906
23	C	-0.242	-0.243	-0.224	-0.224	-0.238	-0.238	3.947	3.947	3.941	3.939	3.946	3.945
24	C	0.828	0.825	0.828	0.826	0.828	0.824	3.822	3.824	3.815	3.818	3.821	3.823
25	C	-0.777	-0.775	-0.780	-0.778	-0.778	-0.775	3.822	3.823	3.815	3.816	3.821	3.822
26	C	0.834	0.829	0.835	0.831	0.835	0.829	3.820	3.823	3.812	3.815	3.818	3.821
27	C	-0.776	-0.775	-0.780	-0.778	-0.777	-0.776	3.825	3.824	3.817	3.817	3.823	3.823
28	H	0.270	0.270	0.255	0.256	0.303	0.304	0.931	0.931	0.938	0.938	0.912	0.912
29	H	0.250	0.250	0.275	0.276	0.272	0.277	0.940	0.940	0.926	0.926	0.929	0.926
30	H	0.245	0.245	0.255	0.255	0.252	0.252	0.943	0.943	0.937	0.937	0.939	0.939
31	H	0.239	0.239	0.250	0.249	0.275	0.275	0.946	0.946	0.940	0.940	0.928	0.928
32	H	0.249	0.250	0.289	0.289	0.261	0.264	0.940	0.940	0.918	0.918	0.934	0.932
33	H	0.255	0.256	0.290	0.290	0.271	0.273	0.937	0.937	0.917	0.918	0.928	0.927
34	H	0.250	0.250	0.256	0.255	0.251	0.251	0.939	0.939	0.936	0.937	0.939	0.938
35	H	0.205	0.205	0.269	0.268	0.240	0.243	0.963	0.963	0.930	0.930	0.945	0.944
36	H	0.239	0.240	0.269	0.269	0.266	0.270	0.945	0.944	0.929	0.929	0.931	0.929
37	H	0.257	0.258	0.266	0.267	0.265	0.269	0.938	0.938	0.933	0.933	0.934	0.932
38	H	0.234	0.235	0.247	0.247	0.238	0.238	0.947	0.947	0.941	0.941	0.945	0.945
39	H	0.249	0.250	0.269	0.271	0.253	0.256	0.939	0.939	0.929	0.928	0.937	0.936
40	H	0.189	0.190	0.259	0.260	0.229	0.229	0.969	0.968	0.933	0.933	0.949	0.949
41	H	0.226	0.227	0.263	0.263	0.252	0.257	0.950	0.950	0.931	0.931	0.938	0.935
42	H	0.229	0.230	0.265	0.264	0.263	0.268	0.949	0.949	0.931	0.931	0.933	0.930
43	H	0.237	0.236	0.249	0.249	0.239	0.239	0.945	0.946	0.939	0.939	0.944	0.944
44	H	0.247	0.248	0.264	0.266	0.251	0.253	0.940	0.940	0.931	0.931	0.938	0.938
45	H	0.270	0.265	0.272	0.268	0.270	0.265	0.930	0.932	0.928	0.930	0.929	0.932
46	H	0.256	0.257	0.265	0.265	0.257	0.259	0.936	0.935	0.931	0.930	0.935	0.934
47	H	0.253	0.255	0.265	0.266	0.255	0.257	0.938	0.936	0.931	0.930	0.937	0.935
48	H	0.262	0.260	0.268	0.266	0.264	0.263	0.933	0.934	0.929	0.930	0.932	0.932
49	H	0.255	0.257	0.265	0.266	0.257	0.260	0.937	0.935	0.931	0.931	0.935	0.934
50	H	0.257	0.258	0.267	0.267	0.259	0.260	0.936	0.935	0.930	0.930	0.935	0.934
51	H			0.461	0.463	0.410	0.457			0.791	0.789	0.841	0.804
52	Cl					-0.710	-0.811					0.514	0.350

Then, in practically all mapped surface of cationic species is observed blue colour because is form is positively charged indicating regions of electrophilic sites on the five rings and, in particular, on the N-H group. In the hydrochloride species, the strong red coloration is observed on the Cl atom due to their available lone pairs, for which, this species is highly nucleophilic around the Cl atoms but less weak on the C=O groups. Here, slight blue colours, typical of electrophilic sites, are observed on the C-H, CH_2 and N-CH_3 groups that belong to the R3 and R5 rings.

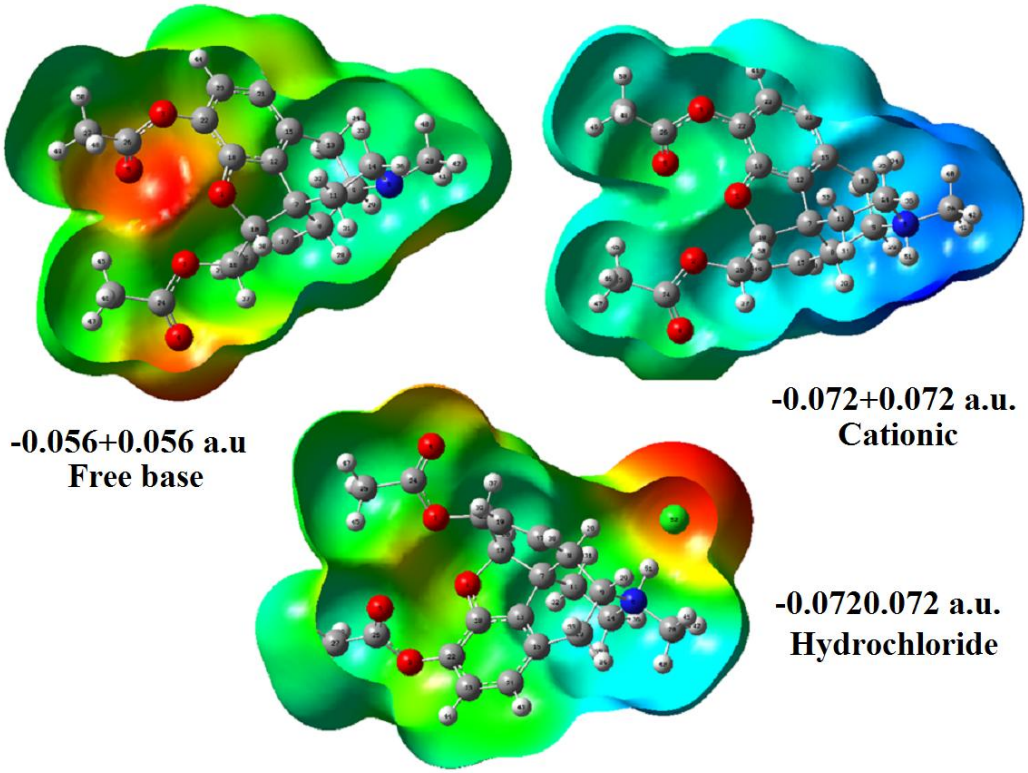

Figure 6. Calculated electrostatic potential surfaces on the molecular surfaces for the three forms of heroin in gas phase. Color ranges indicate in each figure: from red to blue. B3LYP functional and 6-31G* basis set. Isodensity value of 0.005.

Now, if the BOs for the three species are evaluated from Table 4, it is possible to observe that the O2 atoms of free base in both media present the higher values while in the other two species the higher values are observed in the O3 atoms. The higher BO value for the N6 atom is observed in the hydrochloride species due to the presence of Cl atom while the C7 atoms in all species present the higher values than the other ones probably because this atom is common to the R2, R3, R4 and R5 rings of the three species and, as a consequence they are strongly linked in a tetrahedral environmental to four C atoms. In relation to the H atoms, the low BO values are observed in the H51 atoms of cationic and hydrochloride species while for the free base in both media the low BO values are observed in the H28 and H45 atoms. Note that the low BO values for the Cl atoms in the hydrochloride species in both media reveal the ionic characteristics of their halogen H---Cl bonds.

NBO and AIM studies

Due to the multiple biological properties that presents heroin and to its powerful effects [1-8] is useful and necessary to explore their stabilities in both media by using the donor-acceptor

energy interactions and their topological properties by means of the NBO and AIM2000 programs [40,42] at the level B3LYP/6-31G* level of theory. Thus, in **Table 5** are summarized the main donor-acceptor energy interactions for the three heroin species compared with those reported for morphine and cocaine [11,13].

Table 5. Main donor-acceptor energy interactions (in kJ/mol) for the free base, cationic and hydrochloride structures of heroin compared with the corresponding to morphine and cocaine by using the hybrid B3LYP/6-31G* level of theory.

HEROIN						
Delocalization	Free base		Cationic		Hydrochloride	
	Gas	PCM	Gas	PCM	Gas	PCM
*σN6-C9→ LP*H51*					47.40	59.40
*σN6-C14→ LP*H51*					51.50	60.19
*σN6-C20→ LP*H51*					53.50	65.04
$\Delta ET_{\sigma \rightarrow LP^*}$					**152.4**	**184.63**
*π(2)C12-C15→π*C18-C22*	97.35	97.60	43.18	86.27	92.63	92.13
*π(2)C12-C15→π*C21-C23*	74.95	74.70	34.23	68.00	73.61	73.07
*π(2)C18-C22→π*C12-C15*	78.08	77.79	43.81	86.48	81.38	81.63
*π(2)C18-C22→π*C21-C23*	92.54	92.54	45.10	89.70	92.80	92.42
π(2)C21-C23→π C12-C15*	80.71	80.21	43.85	86.61	81.97	81.55
π(2)C21-C23→π C18-C22*	72.73	72.19	37.66	74.99	72.90	72.61
$\Delta ET_{\pi \rightarrow \pi^*}$	**496.36**	**495.03**	**247.83**	**492.05**	**495.29**	**493.41**
*π*C18-C22→π*C12-C15*	806.03	851.59			1146.74	1368.75
*π*C21-C23→π* C12-C15*	812.55	828.31			1136.58	
$\Delta ET_{\pi^* \rightarrow \pi^*}$	**1618.58**	**1679.9**			**2283.32**	**1368.75**
LP(2)O1 → π C18-C22*	121.14	120.59	60.61	120.13	122.93	122.18
LP(2)O2 → π O4-C24*	206.91	211.21	94.17	200.64	202.27	206.70
LP(2)O3 → π O5-C26*	180.49	183.38	82.14	175.35	176.98	180.07
$\Delta ET_{LP \rightarrow \pi^*}$	**508.54**	**515.18**	**236.92**	**496.12**	**502.18**	**508.95**
LP(2)O4 → σ O2-C24*	143.92	138.32	75.91	142.16	145.76	139.95
LP(2)O4 → σ C24-C25*	78.46	75.61	37.95	73.48	78.12	75.41
LP(2)O5 → σ O3-C26*	159.84	153.40	84.48	157.00	161.89	154.99
LP(2)O5 → σ C26-C27*	78.04	74.78	37.45	72.27	77.25	74.19
$\Delta ET_{LP \rightarrow \sigma^*}$	**460.26**	**442.11**	**235.79**	**444.91**	**463.02**	**444.54**
σO3-C26→σ O3-C22*			71.94			
			71.94			

*LP(1)N6 → LP*H51*					1233.81	1473.53
*LP(4)Cl52→ LP*H51*					690.91	299.54
$\Delta ET_{LP\rightarrow LP^*}$					**1924.72**	**1773.07**
ΔE_{Total}	**3083.74**	**3132.22**	**792.48**	**1433.08**	**5715.93**	**4648.12**

MORPHINE

Delocalization	Freebase		Cationic		Hydrochloride	
	Gas	PCM	Gas	PCM	Gas	PCM
*σN4-C7→ LP*H41*					47.38	59.36
*σN4-C12→ LP*H41*					51.58	59.20
*σN4-C18→ LP*H41*					54.00	65.10
$\Delta ET_{\sigma\rightarrow LP^*}$					**152.96**	**183.66**
*π(2)C10-C13→π*C16-C20*	89.90	88.15	77.04	78.37	85.74	84.12
*π(2)C10-C13→π*C19-C21*	81.16	79.25	73.96	72.30	79.66	78.71
*π(2)C16-C20→π*C10-C13*	87.61	87.36	97.76	95.56	91.02	90.40
*π(2)C16-C20→π*C19-C21*	78.79	81.04	75.38	77.79	78.58	78.46
π(2)C19-C21→π C10-C13*	73.22	73.80	77.75	79.16	73.76	74.26
π(2)C19-C21→π C16-C20*	78.29	76.38	78.79	78.42	78.08	77.83
$\Delta ET_{\pi\rightarrow\pi^*}$	**488.97**	**485.97**	**480.69**	**481.60**	**486.84**	**483.77**
π C16-C20→π*C10-C13*	764.44	896.73			1040.46	1069.04
π C19-C21→π*C10-C13*	950.27	992.66				
$\Delta ET_{\pi^*\rightarrow\pi^*}$	**1714.71**	**1889.39**			**1040.46**	**1069.04**
LP(2)O1 → π C16-C20*	97.51	103.42	92.10	102.96	100.09	99.13
LP(2)O3 → π C16-C20*	111.28	106.29	126.34	116.19	114.65	110.53
$\Delta ET_{LP\rightarrow\pi^*}$	**208.79**	**209.71**	**218.44**	**219.15**	**214.74**	**209.66**
*LP(1)N4 → LP*H41*					1238.02	1473.60
*LP(4)Cl42→ LP*H41*					669.88	291.08
$\Delta ET_{LP\rightarrow LP^*}$					**1907.90**	**1764.67**
ΔE_{Total}	**2412.47**	**2585.07**	**699.13**	**700.75**	**3802.91**	**3710.81**

COCAINE

Delocalization	Freebase		Cationic		Hydrochloride	
	Gas	PCM	Gas	PCM	Gas	PCM
*σN5-C6→ LP*H44*					44.81	54.30
*σN5-C7→ LP*H44*					58.94	60.99
*σN5-C13→ LP*H44*					63.54	69.26
$\Delta ET_{\sigma\rightarrow LP^*}$					**167.29**	**184.55**
*π(2)C17-C19→π*O4-C15*	95.55	96.56	110.94	107.51	99.23	102.74
*π(2)C17-C19→π*C18-C20*	87.61	87.32	82.56	82.60	88.45	88.16

*π (2)C17-C19→π*C21-C22*	77.46	77.58	71.27	71.81	76.33	75.45
π (2)C18-C20→π C17-C19*	78.79	78.29	80.51	81.01	77.75	77.08
*π (2)C18-C20→π*C21-C22*	90.20	90.16	89.79	89.66	89.70	89.54
π (2) C21-C22→π C17-C19*	92.88	93.30	101.53	100.19	94.26	95.51
*π (2) C21-C22→π*C18-C20*	76.12	75.95	73.23	73.86	76.20	76.03
$\Delta ET_{\pi\rightarrow\pi^*}$	**598.62**	**599.16**	**609.82**	**606.64**	**601.92**	**604.51**
*π*O4-C15→π* C17-C19*	385.94	384.27	279.22	260.08	304.01	287.33
π C17-C19→π*C18-C20*			890.55	890.88		
$\Delta ET_{\pi^*\rightarrow\pi^*}$	**385.94**	**384.27**	**1169.77**	**1150.96**	**304.01**	**287.33**
*LP(2)O1 → σ*O4-C15*	205.36	210.13	165.15	183.13	194.29	36.41
*LP(2)O2 → σ*O3-C14*	200.97	209.04	264.05	250.09	200.47	206.49
*LP(2)O3 → σ*O2-C14*	145.34	137.69	118.59	124.77	140.78	136.39
*LP(2)O3 → σ*N5-C14*			75.16	42.85		
*LP(2)O3 → σ*C8-C14*	81.64	78.63	56.85	64.54	88.57	89.12
*LP(2)O4 → σ*O1-C15*	137.02	132.13	152.49	141.49	139.03	134.60
*LP(2)O4 → σ*C15-C17*	75.24	73.28	70.73	70.68	73.53	72.19
$\Delta ET_{LP\rightarrow\sigma^*}$	**845.57**	**840.89**	**903.01**	**877.55**	**836.67**	**675.20**
*LP(1)N5 → LP*H44*					1323.30	1540.71
*LP(4)Cl45→ LP*H44*					494.24	244.49
$\Delta ET_{LP\rightarrow LP^*}$					**1817.54**	**1785.20**
ΔE_{Total}	**1830.13**	**1824.32**	**2682.60**	**2635.15**	**3727.43**	**3536.79**

The total energy values show clearly that the hydrochloride species of heroin in both media are highly stables with highest values than the corresponding to morphine and cocaine and, then, similar results are observed for the free base of heroin although with lower energy values. However, the cationic species of cocaine are most stable, with practically similar values in both media, than the corresponding to heroin and morphine. Besides, the cationic species of heroin in solution shows a rare and high stability not observed in the morphine and cocaine species, as compared with the value in gas phase. Obviously, these studies clearly support the high stabilities of those three heroin species against to the corresponding to morphine and cocaine.

The Bader's theory of atoms in molecules is very interesting to analyze all types of inter- and intra-molecular interactions, such as ionic, covalent, H bonds and halogen bonds interactions [43]. Hence, the AIM2000 program [42] was employed to compute the topological properties of those three heroin species in the bond critical points (BCPs), ring critical points (RCPs) and, in both media by using the B3LYP/6-31G* level of theory. Thus, in the BCPs and RCPs

of all heroin species were calculated the electron density, $\rho(r)$, the Laplacian values, $\nabla^2\rho(r)$, the eigenvalues $(\lambda 1, \lambda 2, \lambda 3)$ of the Hessian matrix and, the $|\lambda 1|/\lambda 3$ ratio. These properties in both media can be easily seen in **Tables 6** and **7** compared with the reported for morphine and cocaine while in **Figures 7, 8** and **9** are perfectly observed the molecular graphics of those three heroin species in gas phase with the different H bonds (H---H, O---O, H---O), BCPs, RCPs and the new RCPs identified. Obviously, the three heroin species have the five own RCPs which are identified in those figures as R1, R2, R3, R4 and R5 and, where R5 corresponds to tropane ring. For the free base of heroin in gas phase, there are two O5...H45 and O2...O5 interactions and two RCPs new, N1 and N2 (fig. 7) while in solution appears a new H34...H40 interaction. Hence, due to higher number of interactions, the heroin free base is most stable than morphine and cocaine ones. But, the higher topological parameters observed for the tropane ring R3 of morphine, in both media; indicate that the effect of two acetyl groups in heroin is to reduce those properties.

Table 6. Analysis of the topological properties for the free base and cationic structures of heroin compared with the corresponding to morphine and cocaine by using the hybrid B3LYP/6-31G* level of theory.

Free base /HEROIN/Gas							
Parameter (a.u.)	**O5---H45/N1**	**O2---O5/N2**	**RCP1**	**RCP2**	**RCP3**	**RCP4**	**RCP5**
$\rho(r_c)$	0,0040/0,0026	0,0036/0,0026	0,0174	0,0427	0,0185	0,0203	0,0182
$\nabla^2\rho(r_c)$	0,0160/0,0132	0,0176/0,0164	0,1162	0,3042	0,1204	0,1604	0,1192
λ_1	-0,0038/-0,0021	-0,0032/-0,0021	-0,0117	-0,0460	-0,0132	-0,0149	-0,0122
λ_2	-0,0035/0,0042	-0,0027/0,0050	0,0563	0,1627	0,0547	0,0752	0,0619
λ_3	0,0235/0,0113	0,0236/0,0133	0,0716	0,1875	0,0792	0,1000	0,0694
$\lvert\lambda_1\rvert/\lambda_3$	0,1617/0.1858	0.1356/0.1579	0,1634	0,2453	0,1667	0,1490	0,1758
Distance (Å)	2.825	3.282					
Free base/PCM							
Parameter (a.u.)	**O5---H45/N1**	**O2---O5/N2**	**H34---H40/N3**	**RCP1/RCP2**	**RCP3**	**RCP4**	**RCP5**
$\rho(r_c)$	0,0023/0,0020	0,0038/0,0031	0,0107/0,0105	0,0177/0,0420	0,0185	0,0203	0,0181
$\nabla^2\rho(r_c)$	0,0104/0,010	0,0181/0,0181	0,0438/0,0490	0,1184/0,2984	0,1212	0,1600	0,1182
λ_1	-0,0020/-0,0016	-0,0033/-0,0026	-0,0105/-0,0089	-0,0117/-0,0455	-0,0131	-0,0148	-0,0125
λ_2	-0,0017/0,0028	-0,0029/0,0054	-0,0041/0,0047	0,0582/0,1602	0,0558	0,0758	0,0604
λ_3	0,0140/0,0093	0,0244/0,0153	0,0584/0,0532	0,0718/0,1838	0,0784	0,0989	0,0703
$\lvert\lambda_1\rvert/\lambda_3$	0.1428/0.1720	0.1352/0.1699	0.1798/0.1673	0.1629/0.2475	0,1671	0,1496	0,1778
Distance (Å)	3.056	3.260	2.120				
Cation/HEROIN/Gas							
Parameter (a.u.)	**O5---H45/N1**	**O2---O5/N2**	**H34---H40/N3**	**RCP1/RCP2**	**RCP3**	**RCP4**	**RCP5**

$\rho(r_c)$	0.0029/ 0.0023	0.0041/0.0031	0.0097/0.0097	0.0174/0.0426	0.0186	0.0203	0.0177
$\nabla^2\rho(r_c)$	0.0124/0.0120	0.0192/0.0184	0.0412/0.0432	0.01160/0.3052	0.1212	0.1600	0.1100
λ_1	-0.0026/-0.0019	-0.0037/-0.0026	-0.0087/-0.0079	-0.0116/-0.0460	-0.0135	-0.0148	-0.0125
λ_2	-0.0023/0.0037	-0.0032/0.0059	-0.0022/0.0025	0.0558/0.1656	0.0530	0.0747	0.0596
λ_3	0.0174/0.0101	0.0261/0.0150	0.0520/0.0486	0.0719/0.1855	0.0816	0.1003	0.0629
$\lvert\lambda_1\rvert/\lambda_3$	0.1494/0.1881	0.1417/0.1733	0.1673/0.1625	0.1613/0.2479	0.1654	0.1476	0.1987
Distance (Å)	2.962	3.227	2.153				

Cation/PCM

Parameter (a.u.)	**O5---H45/N1**	**O2---O5/N2**	**H34---H40/N3**	**RCP1/RCP2**	**RCP3**	**RCP4**	**RCP5**
$\rho(r_c)$	0.00237/0.00205	0.0039/0.0032	0.0102/0.0101	0.0176/0.0420	0.0186	0.0203	0.0179
$\nabla^2\rho(r_c)$	0.0104/0.0106	0.0188/0.0188	0.0428/0.0457	0.1184/0.2992	0.1217	0.1600	0.1120
λ_1	-0.0020/-0.0017	-0.0035/-0.0028	-0.0095/-0.0083	-0.0116/-0.0454	-0.0133	-0.0148	-0.0127
λ_2	-0.0017/0.0028	-0.0030/0.0056	-0.0031/0.0035	0.0582/0.1615	0.0544	0.0757	0.0598
λ_3	0.0141/0.0094	0.0252/0.0161	0.0554/0.0505	0.0717/0.1830	0.0806	0.0992	0.0647
$\lvert\lambda_1\rvert/\lambda_3$	0.1418/0.1808	0.1388/0.1739	0.1746/0.1643	0.1618/0.2480	0,1650	0,1492	0,1963
Distance (Å)	3.054	3.243	2.126				

Free base/MORPHINE/Gas

Parameter (a.u.)	**O1---H39**	**RCPN**	**RCP1**	**RCP2**	**RCP3**	**RCP4**	**RCP5**
$\rho(r_c)$	0.0218	0.0203	0.0177	0.0414	0.0181	0.0184	0.0204
$\nabla^2\rho(r_c)$	0.0814	0.1096	0.1181	0.2944	0.1188	0.1206	0.1609
λ_1	-0.0260	-0.0197	-0.0116	-0.0451	-0.0122	-0.0131	-0.0147
λ_2	-0.0178	0.0248	0.0575	0.1581	0.0615	0.0545	0.0748
λ_3	0.1252	0.1045	0.0721	0.1814	0.0695	0.0791	0.1008
$\lvert\lambda_1\rvert/\lambda_3$	0.2077	0.1885	0.1609	0.2486	0.1755	0.1656	0.1458
Distance (Å)	2.097						

Free base/PCM

Parameter (a.u.)	**H28---H34**	**RCPN**	**RCP1**	**RCP2**	**RCP3**	**RCP4**	**RCP5**
$\rho(r_c)$	0.0107	0.0105	0.0179	0.0415	0.0181	0.0184	0.0203
$\nabla^2\rho(r_c)$	0.0438	0.0492	0.1198	0.2951	0.1178	0.1208	0.1600
λ_1	-0.0106	-0.0089	-0.0116	-0.0449	-0.0125	-0.0129	-0.0146
λ_2	-0.0043	0.0049	0.0593	0.1582	0.0598	0.0557	0.0743
λ_3	0.0586	0.0531	0.0720	0.1819	0.0704	0.0780	0.1000
$\lvert\lambda_1\rvert/\lambda_3$	0.1809	0.1676	0.1611	0.2468	0.1776	0.1654	0.1460
Distance (Å)	2.117						

Cation/ MORPHINE Gas

Parameter (a.u.)			**RCP1**	**RCP2**	**RCP3**	**RCP4**	**RCP5**
$\rho(r_c)$			0.0166	0.0434	0.0177	0.0186	0.0166
$\nabla^2\rho(r_c)$			0.1104	0.3092	0.1100	0.1207	0.1104
λ_1			-0.0119	-0.0447	-0.0123	-0.0139	-0.0119
λ_2			0.0522	0.1646	0.0598	0.0514	0.0522
λ_3			0.0700	0.1893	0.0625	0.0831	0.0700
$\lvert\lambda_1\rvert/\lambda_3$			0.1700	0.2361	0.1968	0.1673	0.1700

Cation/PCM

Parameter (a.u.)	H28---H34	RCPN	RCP1	RCP2	RCP3	RCP4	RCP5
$\rho(r_c)$	0.0104	0.0102	0.0177	0.0415	0.0179	0.0186	0.0203
$\nabla^2\rho(r_c)$	0.0434	0.0468	0.1194	0.2958	0.1117	0.1216	0.1600
λ_1	-0.0098	-0.0084	-0.0115	-0.0448	-0.0127	-0.0132	-0.0147
λ_2	-0.0036	0.0042	0.0591	0.1594	0.0597	0.0541	0.0743
λ_3	0.0569	0.0510	0.0717	0.1812	0.0647	0.0805	0.1003
$\lvert\lambda_1\rvert/\lambda_3$	0.1722	0.1647	0.1604	0.2472	0.1963	0.1640	0.1466
Distance (Å)	2.113						

Free base/COCAINE/Gas

Parameter (a.u.)	O3---H31	RCPN	RCP1	RCP2	RCP3
$\rho(r_c)$	0.0082	0.0080	0.0202	0.0194	0.0393
$\nabla^2\rho(r_c)$	0.0316	0.0348	0.1617	0.1252	0.2660
λ_1	-0.0069	-0.0052	-0.0152	-0.0131	-0.0399
λ_2	-0.0036	0.0043	0.0878	0.0595	0.1489
λ_3	0.0422	0.0356	0.0892	0.0787	0.1569
$\lvert\lambda_1\rvert/\lambda_3$	0.1635	0.1461	0.1704	0.1665	0.2543
Distance (Å)	2.627				

Free base/PCM

Parameter (a.u.)	O3---H31	RCPN	RCP1	RCP2	RCP3
$\rho(r_c)$	0.0074	0.0074	0.0201	0.0193	0.0395
$\nabla^2\rho(r_c)$	0.0294	0.0307	0.1612	0.1236	0.2654
λ_1	-0.0059	-0.0053	-0.0152	-0.0133	-0.0402
λ_2	-0.0014	0.0016	0.0873	0.0587	0.1469
λ_3	0.0367	0.0343	0.0890	0.0782	0.1586
$\lvert\lambda_1\rvert/\lambda_3$	0.1608	0.1545	0.1708	0.1701	0.2535
Distance (Å)	2.690				

Cation/ COCAINE/Gas

Parameter (a.u.)	O3---H44	RCPN	RCP1	RCP2	RCP3
$\rho(r_c)$	0.0419	0.0165	0.0201	0.0188	0.0374
$\nabla^2\rho(r_c)$	0.1304	0.0989	0.1614	0.1164	0.2535
λ_1	-0.0645	-0.0123	-0.0152	-0.0127	-0.0372
λ_2	-0.0631	0.0479	0.0877	0.0551	0.1442
λ_3	0.2580	0.0632	0.0889	0.0741	0.1465
$\lvert\lambda_1\rvert/\lambda_3$	0.2500	0.1946	0.1710	0.1714	0.2539
Distance (Å)	1.778				

Cation/PCM

Parameter (a.u.)	O3---H44	RCPN1	C19---H38	RCPN1	RCP1	RCP2	RCP3
$\rho(r_c)$	0.0298	0.0145	0.0005	0.0005	0.0201	0.0188	0.0377
$\nabla^2\rho(r_c)$	0.0894	0.0827	0.0021	0.0025	0.1612	0.1174	0.2563
λ_1	-0.0402	-0.0104	-0.0002	-0.0001	-0.0152	-0.0128	-0.0378
λ_2	-0.0388	0.0378	-0.0001	0.0002	0.0872	0.0559	0.1455
λ_3	0.1685	0.0553	0.0024	0.0024	0.0891	0.0743	0.1485

$\lvert\lambda_1\rvert/\lambda_3$	0.2386	0.1881	0.0833	0.0417	0.1706	0.1723	0.2545
Distance (Å)	1.942		4.038				

Table 7. Analysis of the topological properties for the hydrochloride structures of morphine and cocaine by using the hybrid B3LYP/6-31G* level of theory.

Hydrochloride/HEROIN/GAS											
Parameter (a.u.)	O5---H45/N1	O2---O5/N2	Cl52---H28	Cl52---H51	N3	Cl52---H31/N4	RCP1	RCP2	RCP3	RCP4	RCP5
$\rho(r_c)$	0.0051/0.0029	0.0038/0.0027	0.0101	0.0736	0.0095	0.0063/0.0062	0.0172	0.0428	0.0186	0.0203	0.0179
$\nabla^2\rho(r_c)$	0.0196/0.0148	0.0184/0.0162	0.0316	0.0948	0.0366	0.0202/0.0220	0.1148	0.3056	0.1216	0.1603	0.1136
λ_1	-0.0049/-0.0024	-0.0034/-0.0020	-0.0081	-0.1194	-0.0076	-0.0038/-0.0034	-0.0118	-0.0459	-0.0136	-0.0149	-0.0126
λ_2	-0.0046/0.0047	-0.0028/0.0051	-0.0051	-0.1193	0.0056	-0.0016/0.0020	0.0547	0.1646	0.0533	0.0750	0.0608
λ_3	0.0291/0.0126	0.0245/0.0131	0.0449	0.3336	0.0386	0.0257/0.0233	0.0720	0.1870	0.0818	0.1002	0.0653
$\lvert\lambda_1\rvert/\lambda_3$	0.1684/0.1904	0.1388/0.1527	0.1804	0.3579	0.1969	0.1479/0.1459	0.1639	0.2455	0.1663	0.1487	0.1930
Distance (Å)	2.723	3.261	2.781	1.755		3.055					
Hydrochloride/ HEROIN/PCM											
Parameter (a.u.)	O5---H45/N1	O2---O5/N2		Cl52---H51	H34---H40	N3	RCP1	RCP2	RCP3	RCP4	RCP5
$\rho(r_c)$	0.0022/0.0019	0.0038/0.0031		0.0412	0.0104	0.0103	0.0176	0.0420	0.0186	0.0203	0.0178
$\nabla^2\rho(r_c)$	0.0098/0.0101	0.0183/0.0183		0.0767	0.0436	0.0467	0.1180	0.2993	0.1220	0.1600	0.1116
λ_1	-0.0019/-0.0016	-0.0034/-0.0027		-0.0525	-0.0095	-0.0084	-0.0117	-0.0456	-0.0134	-0.0148	-0.0127
λ_2	-0.0016/0.0026	-0.0029/0.0054		-0.0523	-0.0029	0.0032	0.0575	0.1616	0.0546	0.0758	0.0596
λ_3	0.0134/0.0090	0.0246/0.0155		0.1817	0.0560	0.0518	0.0720	0.1833	0.0806	0.0992	0.0647
$\lvert\lambda_1\rvert/\lambda_3$	0.1418/0.1777	0.1382/0.1742		0.2889	0.1696	0.1622	0.1625	0.2488	0.1663	0.1492	0.1963
Distance (Å)	3.079	3.256		2.036	2.133						
Hydrochloride/MORPHINE/GAS											
Parameter (a.u.)	Cl42---H22	RCPN1	Cl42---H25	RCPN2	Cl42---H41	RCPN3	RCP1	RCP2	RCP3	RCP4	RCP5
$\rho(r_c)$	0.0105	0.0098	0.0065	0.0064	0.0724	0.0098	0.0176	0.0414	0.0179	0.0186	0.0204
$\nabla^2\rho(r_c)$	0.0329	0.0380	0.0208	0.0228	0.0957	0.0380	0.1176	0.2947	0.1132	0.1212	0.1608
λ_1	-0.0085	-0.0081	-0.0040	-0.0035	-0.1168	-0.0081	-0.0116	-0.0451	-0.0126	-0.0134	-0.0147
λ_2	-0.0055	0.0058	-0.0019	0.0025	-0.1166	0.0058	0.0569	0.1595	0.0602	0.0534	0.0748
λ_3	0.0469	0.0402	0.0268	0.0238	0.3291	0.0402	0.0723	0.1803	0.0655	0.0812	0.1007
$\lvert\lambda_1\rvert/\lambda_3$	0.1812	0.2015	0.1493	0.1471	0.3549	0.2015	0.1604	0.2501	0.1924	0.1650	0.1460
Distance (Å)	2.760		3.038		1.762						
Hydrochloride/MORPHINE/PCM											
Parameter (a.u.)	H28---H34	RCPN	O1---H39	RCPN2			RCP1	RCP2	RCP3	RCP4	RCP5
$\rho(r_c)$	0.0108	0.0106	0.0207	0.0198			0.0176	0.0414	0.0178	0.0185	0.0203
$\nabla^2\rho(r_c)$	0.0450	0.0490	0.0800	0.1042			0.1178	0.2948	0.1117	0.1216	0.1602
λ_1	-0.0104	-0.0086	-0.0237	-0.0187			-0.0117	-0.0449	-0.0126	-0.0132	-0.0147
λ_2	-0.0044	0.0052	-0.0143	0.0192			0.0574	0.1597	0.0591	0.0547	0.0742
λ_3	0.0596	0.0524	0.1182	0.1036			0.0720	0.1799	0.0652	0.0801	0.1007
$\lvert\lambda_1\rvert/\lambda_3$	0.1745	0.1641	0.2005	0.1805			0.1625	0.2496	0.1933	0.1648	0.1460
Distance (Å)	2.101		2.133								

Hydrochloride/COCAINE/GAS											
Parameter (a.u.)	O3---O1	RCPN1	Cl45---H31	RCPN2	Cl45---H37	RCPN3	Cl45---H44	RCPN4	RCP1	RCP2	RCP3
$\rho(r_c)$	0.0143	0.0126	0.0105	0.0092	0.0083	0.0061	0.0603	0.0092	0.0202	0.0189	0.0381
$\nabla^2\rho(r_c)$	0.0501	0.0629	0.0341	0.0376	0.0276	0.0253	0.0984	0.0376	0.1617	0.1186	0.2580
λ_1	-0.0124	-0.0100	-0.0086	-0.0068	-0.0067	-0.0039	-0.0906	-0.0068	-0.0152	-0.0127	-0.0377
λ_2	-0.0109	0.0172	-0.0064	0.0080	-0.0062	0.0058	-0.0900	0.0080	0.0879	0.0553	0.1459
λ_3	0.0734	0.0557	0.0492	0.0363	0.0405	0.0234	0.2789	0.0363	0.0891	0.0759	0.1498
$\lvert\lambda_1\rvert/\lambda_3$	0.1689	0.1795	0.1748	0.1873	0.1654	0.1667	0.3248	0.1873	0.1706	0.1673	0.2517
Distance (Å)	2.750		2.744		2.838		1.843				
Hydrochloride/ COCAINE/PCM											
Parameter (a.u.)	O3---O1	RCPN1	Cl45---H31	RCPN2	Cl45---H37	RCPN3	Cl45---H44	RCPN4	RCP1	RCP2	RCP3
$\rho(r_c)$	0.0141	0.0126			0.0034	0.0027	0.0369	0.0027	0.0201	0.0188	0.0380
$\nabla^2\rho(r_c)$	0.0487	0.0616			0.0100	0.0107	0.0728	0.0107	0.1612	0.1176	0.2578
λ_1	-0.0126	-0.0095			-0.0023	-0.0006	-0.0453	-0.0006	-0.0152	-0.0128	0.0375
λ_2	-0.0105	0.0164			-0.0021	0.0026	-0.0451	0.0026	0.0873	0.0545	0.1450
λ_3	0.0718	0.0548			0.0144	0.0087	0.1632	0.0087	0.0889	0.0758	0.1502
$\lvert\lambda_1\rvert/\lambda_3$	0.1755	0.1734			0.1597	0.0690	0.2776	0.0690	0.1710	0.1689	-0.2497
Distance (Å)	2.755		3.153		3.309		2.088				

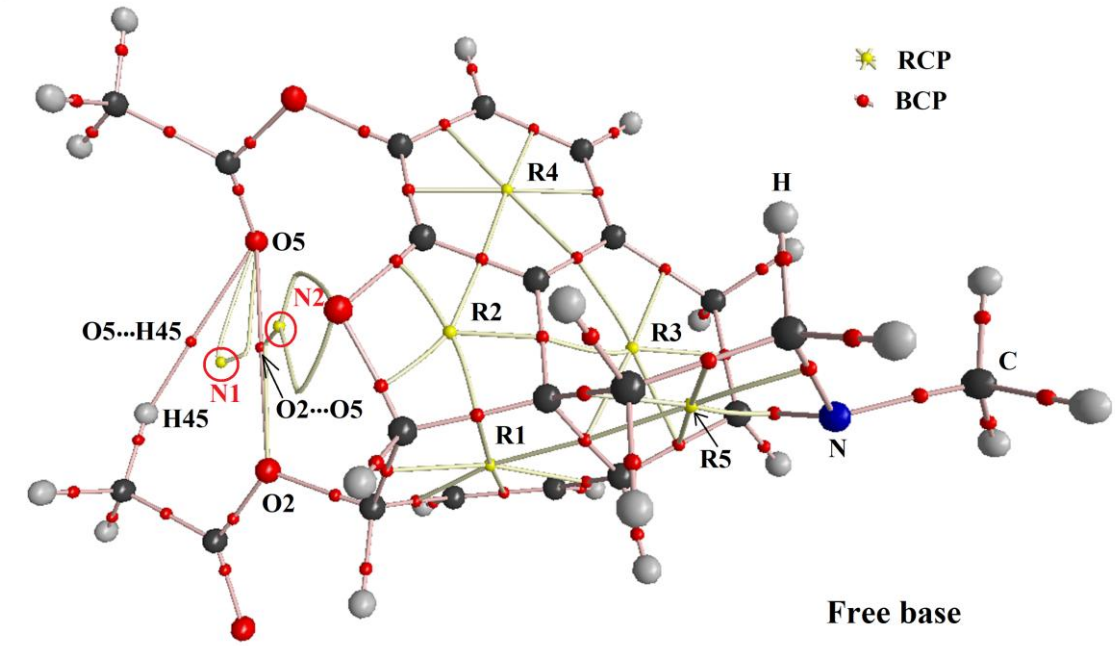

Figure 7. Details of the molecular model for the free base of heroin in gas phase showing the geometry of all their bond critical points (BCPs) and ring critical points (RCPs) at the B3LYP/6-31G* level of theory.

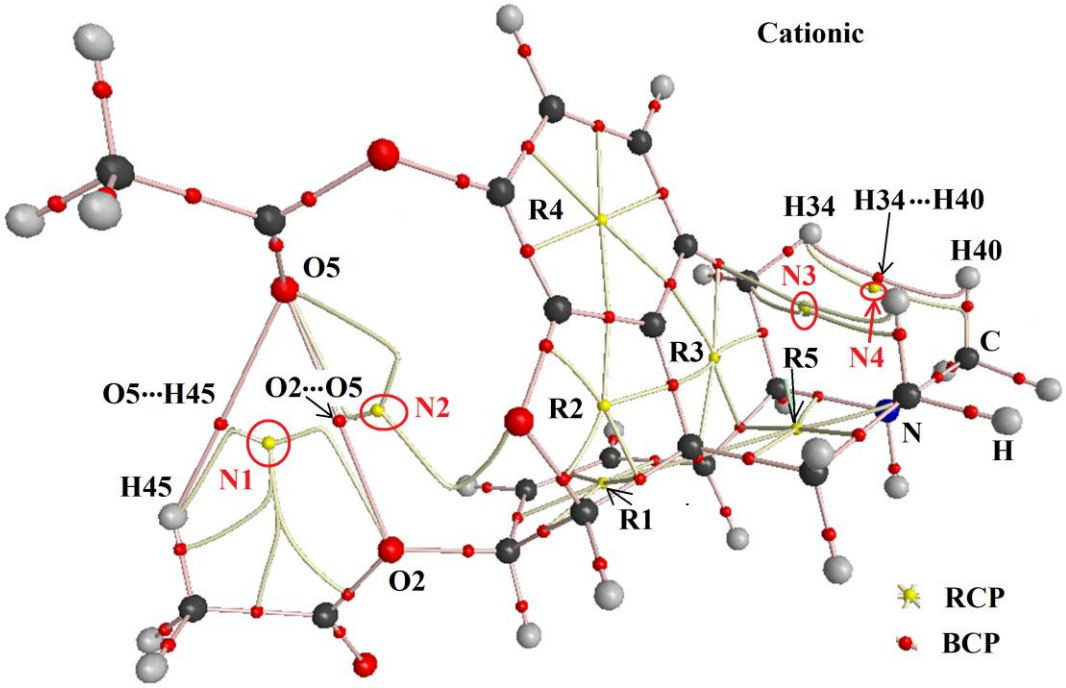

Figure 8. Details of the molecular model for the cationic form of heroin in gas phase showing the geometry of all their bond critical points (BCPs) and ring critical points (RCPs) at the B3LYP/6-31G* level of theory.

Analyzing the cationic heroin, there are observed three O5...H45, O2...O5 and H34...H40 interactions and four new RCPs in both media indicating clearly its higher stability against to morphine and cocaine ones. The hydrochloride heroin species are clearly most stable than the morphine and cocaine ones due to the observed five new interactions in gas phase and only four in solutions. Table 7 shows that the topological properties for the tropane rings of heroin and morphine have practically the same values although the number of interactions favours clearly to heroin. Here, the cocaine species present lower numbers of interactions and RCPs and, for these reasons, are the most unstable species. Hence, these AIM studies support evidently the higher stabilities of the three forms of heroin, as compared with those observed for morphine and cocaine.

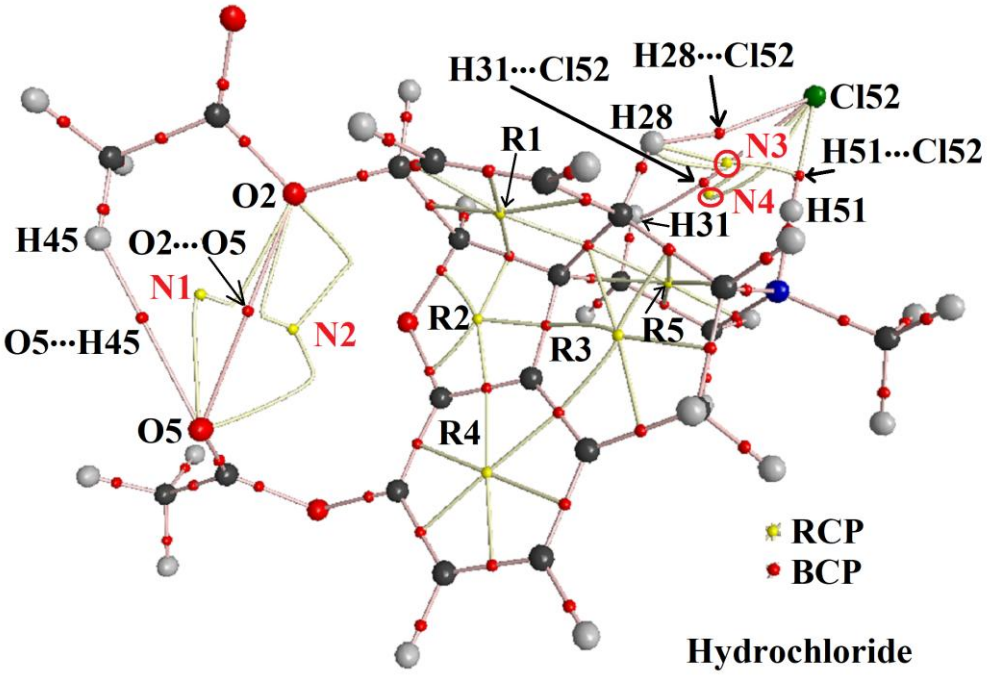

Figure 9. Details of the molecular model for the hydrochloride form of heroin in gas phase showing the geometry of all their bond critical points (BCPs) and ring critical points (RCPs) at the B3LYP/6-31G* level of theory.

Frontier orbitals and global descriptors studies

The above NBO and AIM studies have revealed that the free base and hydrochloride species of heroin are most stable than those corresponding to morphine and cocaine, however, the cationic cocaine species is most stable in the two media than corresponding to morphine and heroin. Hence, it is very important to analyze and know why the cationic form of cocaine is most stable than those corresponding to heroin and morphine. These differences could probably be explained if the reactivities and behaviours for those three heroin species are analyzed in both media by using the frontier orbitals and some global descriptors [23-30]. Consequently, for the free base, cationic and hydrochloride structures of heroin the HOMO and LUMO, energy band gap [23,24], chemical potential (μ), electronegativity (χ), global hardness (η), global softness (S), global electrophilicity index (ω) and global nucleophilicity index (E) [25-30] were calculated. Thus, in **Table 8** those parameters for all heroin species computed in both media by using the hybrid B3LYP/6-31G* level of theory are presented together with the corresponding to morphine, cocaine and tropane alkaloids [11-13]. Then, the behaviours of all these tropane alkaloids in both media can be easily seen in **Figures 10, 11** and **12**. Analyzing first the HOMO, LUMO and Gap values for the free base, it is

observed that cocaine in both media present the most negative HOMO and LUMO values and low gap values while tropane alkaloid in both media has the highest positive LUMO and gap values. Thus, the tropane alkaloid presents most negative HOMO and most positive gap values than the other ones while the LUMO values are practically similar in all alkaloids. Here, the cationic species of morphine is the most reactive than the other ones but cation heroin is most reactive than cation cocaine. In these cationic species, the behaviors of all descriptors are comparable in all alkaloids with exception of global nucleophilicity index (E) for tropane alkaloid that notably presents the lower values than the other ones.

Table 8. Calculated HOMO and LUMO orbitals, energy band gap, chemical potential (*μ*), electronegativity (*χ*), global hardness (*η*), global softness (*S*), global electrophilicity index (*ω*) and global nucleophilicity index (E) for the free base, cationic and hydrochloride structures of morphine, cocaine and tropane by using the hybrid B3LYP/6-31G* level of theory.

HEROIN[a]						
Frontier orbitals (eV)	Free base		Cationic		Hydrochloride	
	Gas	PCM	Gas	PCM	Gas	PCM
HOMO	-5.7490	-5.7471	-8.7639	-8.7907	-5.8841	-5.1808
LUMO	-0.0927	-0.1057	-3.3371	-3.4150	-0.5817	-0.7339
|GAP|	5.6563	5.6414	5.4268	5.3757	5.3024	4.4469
Descriptors (eV)						
χ	-2.8282	-2.8207	-2.7134	-2.6879	-2.6512	-2.2235
μ	-2.9209	-2.9264	-6.0505	-6.1029	-3.2329	-2.9574
η	2.8282	2.8207	2.7134	2.6879	2.6512	2.2235
S	0.1768	0.1773	0.1843	0.1860	0.1886	0.2249
ω	1.5083	1.5180	6.7459	6.9284	1.9711	1.9667
E	-8.2606	-8.2545	-16.4174	-16.4035	-8.5711	-6.5755
MORPHINE[b]						
Frontier orbitals (eV)	Free base		Cationic		Hydrochloride	
	Gas	PCM	Gas	PCM	Gas	PCM
HOMO	-5.5670	-5.3367	-8.5413	-8.4347	-5.8917	-5.1973
LUMO	0.0374	0.1383	-3.3524	-3.4103	-0.4500	-0.6133
|GAP|	5.6044	5.4750	5.1889	5.0244	5.4417	4.5840
Descriptors (eV)						
χ	-2.8022	-2.7375	-2.5945	-2.5122	-2.7209	-2.2920
μ	-2.7648	-2.5992	-5.9469	-5.9225	-3.1709	-2.9053
η	2.8022	2.7375	2.5945	2.5122	2.7209	2.2920
S	0.1784	0.1826	0.1927	0.1990	0.1838	0.2182

ω	1.3639	1.2339	6.8155	6.9811	1.8476	1.8414
E	-7.7475	-7.1153	-15.4288	-14.8785	-8.6274	-6.6589

COCAINE[c]

Frontier orbitals (eV)	Free base		Cationic		Hydrochloride	
	Gas	PCM	Gas	PCM	Gas	PCM
HOMO	-5.9267	-6.0125	-9.3162	-9.2302	-5.6938	-4.9833
LUMO	-1.0687	-1.0638	-3.8694	-3.7642	-1.1856	-1.3020
|GAP|	4.858	4.9487	5.4468	5.4660	4.5082	3.6813
Descriptors (eV)						
χ	-2.4290	-2.4744	-2.7234	-2.7330	-2.2541	-1.8407
μ	-3.4977	-3.5382	-6.5928	-6.4972	-3.4397	-3.1427
η	2.4290	2.4744	2.7234	2.7330	2.2541	1.8407
S	0.2058	0.2021	0.1836	0.1829	0.2218	0.2716
ω	2.5183	2.5297	7.9799	7.7229	2.6244	2.6828
E	-8.4959	-8.7546	-17.9548	-17.7568	-7.7534	-5.7845

TROPANE ALKALOID[d]

Frontier orbitals (eV)	Free base		Cationic		Hydrochloride	
	Gas	PCM	Gas	PCM	Gas	PCM
HOMO	-5.4945	-5.6725	-12.9365	-12.9433	-5.5910	-4.9043
LUMO	2.0561	1.9886	-3.3770	-3.4183	1.2336	1.0076
|GAP|	7.5506	7.6611	9.5595	9.5250	6.8246	5.9119
Descriptors (eV)						
χ	-3.7753	-3.8306	-4.7798	-4.7625	-3.4123	-2.9560
μ	-1.7192	-1.8420	-8.1567	-8.1808	-2.1787	-1.9483
η	3.7753	3.8306	4.7798	4.7625	3.4123	2.9560
S	0.1324	0.1305	0.1046	0.1050	0.1465	0.1691
ω	0.3914	0.4429	6.9598	7.0263	0.6955	0.6421
E	-6.4905	-7.0557	-38.9872	-38.9613	-7.4343	-5.7592

$\chi = -[E(LUMO) - E(HOMO)]/2$; $\mu = [E(LUMO) + E(HOMO)]/2$; $\eta = [E(LUMO) - E(HOMO)]/2$;

$S = \frac{1}{2}\eta$; $\omega = \mu^2/2\eta$; $E = \mu * \eta$

[a]This work, [b]From Ref [30], [c]From Ref [31]

Here, heroin and morphine have practically the same behaviours in both media but the HOMO values for heroin in both media are slightly most negative in heroin than in morphine. Here, the free base of heroin is most reactive than morphine but cocaine is the most reactive of all alkaloids while tropane the less reactive. In relation to the descriptors, heroin and morphine present similar behaviours in both media while the higher differences are observed in the values for cocaine and tropane. Thus, the free base of cocaine presents higher electronegativity (χ) and global electrophilicity index (ω) values while lower chemical potential (μ) and global nucleophilicity index (E) than the other alkaloids. If now the cationic

species are analyzed from Figure 8 and Table 10, it is observed analogous behaviors in both media.

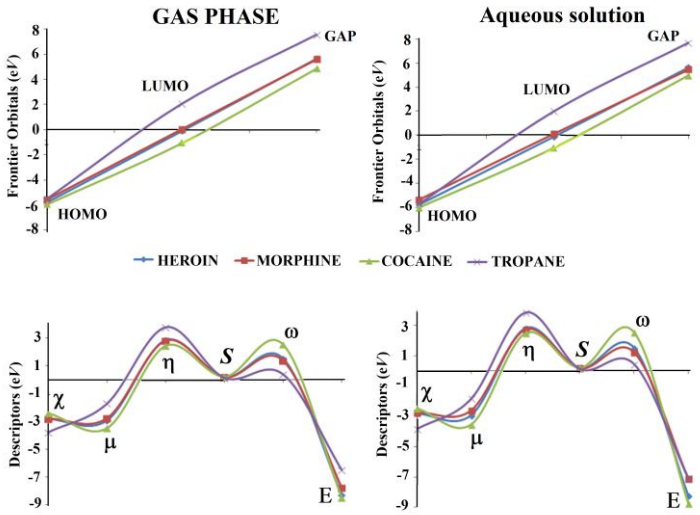

Figure 10. Frontier orbitals (upper) and descriptors values (bottom) for the free base of heroin in gas and aqueous solution phases compared with the corresponding to morphine, cocaine and tropane at the B3LYP/6-31G* level of theory.

Evidently the presence of other groups linked to tropane ring increase significantly the reactivity of alkaloid, specifically of its cationic form. When the hydrochloride species are compared, the lower HOMO, LUMO and gap values are observed for cocaine while the higher values for tropane.

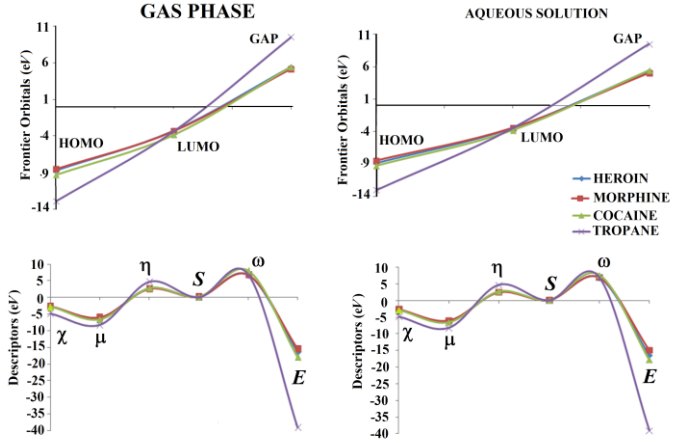

Figure 11. Frontier orbitals (upper) and descriptors values (bottom) for the cationic form of heroin in gas and aqueous solution phases compared with the corresponding to morphine, cocaine and tropane at the B3LYP/6-31G* level of theory.

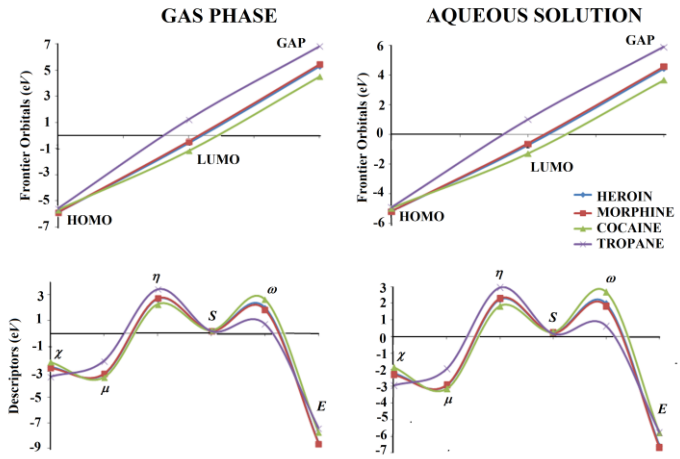

Figure 12. Frontier orbitals (upper) and descriptors values (bottom) for the hydrochloride form of heroin in gas and aqueous solution phases compared with the corresponding to morphine, cocaine and tropane at the B3LYP/6-31G* level of theory.

These forms for heroin and morphine have comparable values but, the hydrochloride heroin form is the most reactive than the other ones while tropane is the least reactive of all alkaloids. Here newly it is evidenced that when other groups are linked to tropane ring the reactivity of alkaloid increases the reactivity of hydrochloride form. The behaviors of descriptors for this form is similar to the free base showing clearly that tropane alkaloid is the less reactive and, for this reason, that species has the most global hardness (η) values in both media. The hydrochloride form of cocaine has higher global electrophilicity index (ω) while the heroin and morphine ones have the lower global nucleophilicity index (E) values. These results could suggest a probable explanation why the hydrochloride heroin form in gas phase is the most reactive than the other ones but in solution, the cocaine species is the most reactive.

Here, the potential pharmacological properties for the three heroin species were analyzed taking into account the rule of five states suggested by Lipinski's and Veber [44,45]. Hence, the three species could present absorption or permeation because: (i) the cationic and hydrochloride species have a only NH group (< number than 5 H-bond donors), (ii) the molecular weights for the three species are between 369.411 and 423.89 g/mol <<< than 500 and, (iii) the three species have only an N and five O atoms H-bond acceptor (< 10 H-bond acceptors). Accordingly, the three heroin species could present potential pharmacological properties, as they are broadly known.

Vibrational analysis

The three heroin species in both media were optimized with C_1 symmetries by using hybrid B3LYP/6-31G* level of theory. The number of normal vibration modes expected for the free base, cationic and hydrochloride structures are 144, 147 and 150, respectively which present activities in both infrared and Raman spectra. The experimental available infrared and Raman spectra for the free base and the hydrochloride forms of heroin in solid state were taken from Ref [18]. Both spectra are compared in **Figures 13** and **14** with the corresponding predicted to the free base, cationic and hydrochloride heroin forms in gas phase by using B3LYP/6-31G* level of theory. Note that very good correlations are observed among experimental and theoretical ones, especially when the Raman activities obtained by the calculations are converted in Raman intensities by using known equations [46,47].

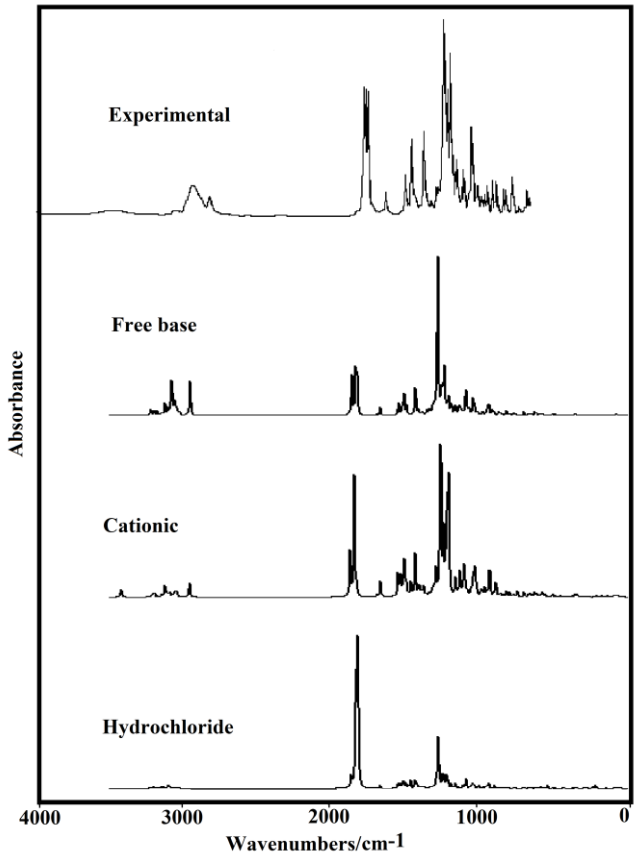

Figure 13. Comparisons between the experimental available FTIR spectrum of hydrochloride form of heroin in the solid state [18] with the corresponding predicted for the free base, cationic and hydrochloride species in the gas phase at B3LYP/6-31G* level of theory.

The most intense band, predicted in the IR spectrum of hydrochloride form at 1817 cm^{-1} which is shifted up to 1746 cm^{-1} by using SQM calculations, is attributed to the N6-H51 and Cl52-H51 stretching modes, in form similar to the observed in morphine [11]. Here, the intensities ratio between the most intense bands in the predicted IR spectrum of hydrochloride form is different from those observed in the experimental spectrum, as observed in Figure 13, indicating probably that the hydrochloride form is present as cationic species, as was also observed in the spectra of morphine and cocaine [11,13]. Obviously, the differences among experimental and theoretical spectra can be in part associated to the calculations performed in gas phase, for the isolated molecules and, also to the packing forces because these forces were not considered here. The SQMFF procedure, the Molvib program, the normal internal coordinates for the three heroin species and scale factors predicted at the 6-31G* level of theory [16] were used to obtain the harmonic force fields. Only, potential energy distribution (PED) contributions ≥ 10 % were considered to perform the complete assignments for the three heroin species. **Table 9** are presented the observed and calculated wavenumbers together with the proposed assignments while the discussions of some assignments by regions are presented below.

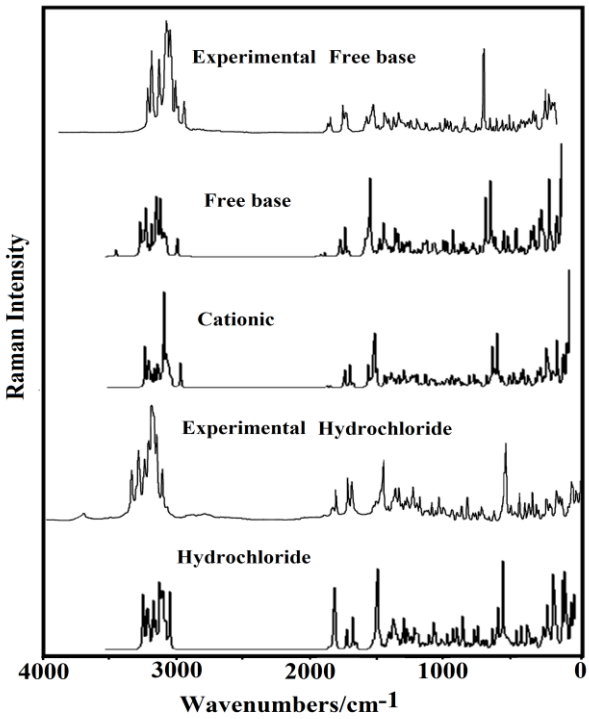

Figure 14. Comparisons between the experimental available Raman spectra of free base and hydrochloride species of heroin in the solid state [18] with the corresponding predicted for the free base, cationic and hydrochloride species in the gas phase at B3LYP/6-31G level of theory**

Table 9. Observed and calculated wavenumbers (cm^{-1}) and assignments for the free base, cationic and hydrochloride species of Heroin in gas phase

Experimental				B3LYP/6-31G* Method[a]					
Freebase		Hydrochloride		Freebase		Cationic		Hydrochloride	
FTIR[c]	Raman[d]	FTIR[c]	Raman[d]	SQM[b]	Assignments	SQM[b]	Assignments	SQM[b]	Assignments
3483vw		3452w	3400w	3078	νC23-H44	3268	νN6-H51	3081	νC23-H44
		3393sh	3082m	3077	νC19-H39	3095	νC19-H39	3080	νC19-H39
3059vw	3060m	3228sh		3055	νC21-H43	3090	νC23-H44	3057	νC21-H43
				3051	ν_aCH_3(C27)	3077	ν_aCH_3(C20)	3053	ν_aCH_3(C27)
			3052sh	3049	ν_aCH_3(C25)	3067	νC21-H43	3051	ν_aCH_3(C25)
			3047sh	3032	νC17-H38	3058	ν_aCH_3(C27)	3047	ν_aCH_3(C20)
	3035s	3041sh	3039m	3007	ν_aCH_3(C27)	3058	ν_aCH_3(C20)	3039	ν_aCH_3(C20)
				3007	ν_aCH_3(C25)	3056	ν_aCH_3(C25)	3035	νC17-H38
	2981s	2996sh	2995m	2985	ν_aCH_3(C20)	3048	νC17-H38	3009	ν_aCH_3(C25)
				2982	νC10-H30	3033	ν_aCH_2(C14)	3008	ν_aCH_3(C27)
	2969sh			2962	ν_aCH_2(C11)	3010	ν_aCH_3(C25)	3008	ν_aCH_2(C14)
2943w	2947sh			2945	ν_sCH_3(C27)	3010	ν_aCH_3(C27)	2994	νC10-H30
				2943	ν_aCH_3(C20)	2988	νC10-H30	2983	ν_aCH_2(C11)
			2969s	2940	ν_sCH_3(C25)	2984	ν_aCH_2(C11)	2963	νC9-H29
			2969s	2940	ν_aCH_2(C14)	2978	ν_sCH_2(C14)	2959	ν_sCH_3(C20)
			2951vs	2939	ν_aCH_2(C13)	2974	ν_sCH_3(C20)	2954	ν_sCH_2(C14)
2924sh	2927vs	2947w	2951vs	2924	νC9-H29	2967	νC9-H29	2951	ν_aCH_2(C13)
			2951vs	2916	νC16-H37	2952	ν_aCH_2(C13)	2946	ν_sCH_3(C27)
	2941sh		2939sh	2914	ν_sCH_2(C11)	2949	ν_sCH_3(C27)	2941	ν_sCH_3(C25)
				2906	ν_sCH_2(C13)	2944	ν_sCH_3(C25)	2936	ν_sCH_2(C11)
						2928	ν_sCH_2(C13)	2923	νC16-H37
		2915sh	2917s			2914	ν_sCH_2(C11)	2920	ν_sCH_2(C13)
2889w	2897vs	2867sh	2879s	2891	νC8-H28	2906	νC16-H37	2894	νC8-H28
2826w	2857s			2826	ν_sCH_2(C14)	2829	νC8-H28		
2808sh	2794s			2819	ν_sCH_3(C20)				
1775s	1757w	1754s	1773w	1785	νC26-O5	1795	νC26-O5	1787	νC26-O5
1755s	1737m	1733vs	1754s	1756	νC24-O4	1767	νC24-O4	1759	νC24-O4
1751sh	1649m		1674s					1746	νN6-H51
1658w	1624m		1645s	1661	νC17-C19	1658	νC17-C19	1664	νC17-C19
1635w			1645s	1626	νC12-C18	1626	νC12-C18νC21-C23	1626	νC12-C18
		1607w		1606	νC18-C22νC12-C15	1604	νC18-C22νC12-C15	1606	νC18-C22νC12-C15
1499w			1498w	1492	βC23-H44νC22-C23 βC21-H43νC15-C21	1497	βC23-H44	1499	ρ'N6-H51 δN6H51Cl52
1490sh		1484m	1484w	1483	δ_aCH_3(C20)			1494	βC23-H44βC21-H43
	1474m			1470	δCH$_2$(C14)	1470	δ_aCH_3(C20)	1469	δ'_aCH_3(C20)δ_aCH_3(C20)
1462sh		1460sh				1462	δ_aCH_3(C20)		
1458m			1459sh			1456	δCH$_2$(C14)	1458	δCH$_2$(C14)
1452sh			1451s	1451	δ_aCH_3(C20)			1448	δCH$_2$(C11)
				1445	δ_aCH_3(C25)			1445	δ_aCH_3(C25)
				1444	δCH$_2$(C11)	1444	δCH$_2$(C11)	1444	νC18-O1
1440sh	1442sh	1439s	1435vs	1442	δCH$_2$(C11)	1442	νC18-O1	1441	δ_aCH_3(C27)δCH$_2$(C14)

1440sh	1442sh	1439s	1435vs	1440	$\delta_a CH_3$(C27)	1440	$\delta_a CH_3$(C25)	1440	$\delta_a CH_3$(C25)
		1439s	1435vs			1437	$\delta_a CH_3$(C27)		
1440sh	1442sh	1439s	1435vs	1439	$\delta_a CH_3$(C25)	1435	$\delta_a CH_3$(C25)		
			1435vs	1436	$\delta_a CH_3$(C27)	1434	δCH_2(C13)	1438	$\delta_a CH_3$(C27)
1428sh	1423m	1425m	1430sh	1427	δCH_2(C13)	1433	$\delta_a CH_3$(C27)	1436	$\delta_a CH_3$(C27)
		1425m	1430sh	1424	$\delta_s CH_3$(C20)	1424	ρ'N6-H51	1434	δCH_2(C13)
		1425m	1430sh			1418	ρN6-H51	1430	ρN6-H51τN6-H51
	1391w	1403w	1403w	1397	wagCH_2(C14)	1404	$\delta_s CH_3$(C20)	1400	$\delta_s CH_3$(C20)
1376m				1393	βC17-H38νC16-C19	1392	βC17-H38 βC19-H39νC16-C19	1396	βC17-H38 βC19-H39νC16-C19
	1387sh		1376sh			1378	wagCH_2(C14)	1388	wagCH_2(C14)
1371sh						1367	wagCH_2(C11)	1375	wagCH_2(C11)
	1367w	1368s		1368	ρC9-H29	1367	$\delta_s CH_3$(C25)νC24-C25	1368	$\delta_s CH_3$(C25)
	1367w	1368s		1367	$\delta_s CH_3$(C25)	1364	νC26-C27	1364	ρC10-H30
				1361	$\delta_s CH_3$(C27)			1362	wagCH_2(C13)
1359w		1360sh		1360	ρC10-H30 wagCH_2(C11)	1363	wagCH_2(C13) νC13-C15	1361	$\delta_s CH_3$(C27)νC26-C27
		1360sh		1358	ρ' C9-H29	1358	ρC10-H30	1356	ρC9-H29
1351sh	1346w		1352m	1352	wagCH_2(C13)	1348	ρC16-H37	1348	ρC16-H37ρC10-H30
				1345	ρC16-H37	1346	ρC9-H29	1342	ρC8-H28
	1331sh	1336m	1331m	1334	νC21-C23νC12-C15	1334	ρC8-H28 ρ' C9-H29	1335	νC21-C23
1326w				1329	ρC8-H28	1330	νC21-C23	1326	ρC16-H37ρ'C8-H28
	1312w	1296w	1309w	1315	ρ'C16-H37ρC16-H37			1313	ρ'C16-H37
	1306sh			1297	ρ'C16-H37ρ'C8-H28	1317	ρ'C10-H30		
1291w	1297sh	1296w	1309w	1291	ρCH_2(C14) ρCH_2(C11)	1298	ρ'C16-H37	1285	ρ'C10-H30
1276w	1277m	1272w	1275m			1277	ρCH_2(C11)	1284	ρCH_2(C11)
1276w	1277m	1272w	1275m	1272	ρ'C10-H30	1274	ρ'C8-H28		
1250sh				1256	ρCH_2(C11)	1256	ρCH_2(C13) νC7-C8	1256	ρCH_2(C13) ρ' C9-H29
			1246sh	1244	ρCH_2(C13)			1245	νC22-C23νC22-O3
1237vs	1241m	1238vs	1234m	1240	νC24-O2δCOO(C24)	1249	νC22-O3νC22-C23		
1237vs		1238vs	1234m	1234	νC22-O3			1236	νC24-O2νC24-C25
						1228	βR_3(A3) βR_1(A4)	1232	ρCH_2(C14)
	1227sh	1224s	1228sh	1226	βR_3(A3)	1226	νC15-C21 βC21-H43 ρCH_2(C14)	1225	νC13-C15
1216s	1217m	1212s	1211w	1216	βR_1(A4)	1219	νC24-O2	1209	ρCH_2(C13)
	1200sh			1202	δCOO(C26)	1204	βR_1(A4)	1201	νC15-C21
1197s	1181sh	1196s	1189m	1191	βR_1(A4)	1198	νC7-C12	1194	νC26-O3
1189sh				1185	βC19-H39	1185	βC19-H39 βC17-H38	1187	βC19-H39βC17-H38
		1175s				1180	δCOO(C26)	1179	βR_1(A4)ρ'CH_3(C20)
1177w	1172w	1175s		1175	ρCH_2(C13)	1169	ρ'CH_3(C20)		
1162w	1151w	1153s	1156w	1153	βR_1(A5)	1149	νC21-C23	1150	νC21-C23βC23-H44
1152w	1141sh	1142sh	1145w	1145	νC21-C23			1142	βR_1(A5) ρCH_3(C20)
1139w	1130w		1131w	1131	ρCH_3(C20)	1133	ρCH_3(C20)		
1127w	1111m	1127m		1120	νC7-C8 βR_2(A1)	1120	βR_1(A5)	1123	νC10-C16
1115w			1110w			1104	νC7-C11	1109	βR_1(A5) ρCH_3(C20)
1103w	1097sh			1097	βR_1(A1)νC7-C11				
1094w	1085sh		1085w	1089	νN6-C20νC7-C10	1094	βR_1(A1)	1098	βR_1(A1)νC7-C11
1074w	1068sh	1075w	1061m	1067	τR_1(A5)	1065	νC16-O2	1067	νC10-C16νC7-C8

1056m				1057	ρCH_3(C25)	1058	τR_1(A3)	1062	ρCH_3(C20)
	1051sh		1055sh	1053	νC16-O2	1056	ρCH_3(C25)	1057	ρCH_3(C25)
	1048sh	1045s		1049	ρ'CH_3(C27)			1050	νC16-O2ρ'CH_3(C25)
				1048	νN6-C14νC8-C9	1049	ρ'CH_3(C27)γCOO(C26)	1049	ρ'CH_3(C27)
1041m	1043w	1035sh	1032w	1039	νN6-C9ρ'CH_3(C20)	1044	βR_1(A5) ρCH_3(C20)	1040	νC8-C9νC9-C13 νC7-C10
	1028w	1017m		1022	νC8-C17	1028	νC8-C9νC7-C10 νC9-C13νC8-C17	1018	νN6-C20νC8-C17
1013w		1017m		1010	ρCH_3(C27)			1012	νC11-C14
		1002m				1005	ρCH_3(C27)		
1006sh	1006sh	1002m		1003	νC18-O1νC13-C15	1002	ρCH_3(C27)	1007	ρCH_3(C27) δCOO(C26)
	997w			991	ρ'CH_3(C25)	994	ρ'CH_3(C25)	997	νN6-C14
989w			982sh			989	γC19-H39νN6-C20	989	ρ'CH_3(C25)
980w	972w	974sh	970w	978	δO2C16C19 δO2C16C10	984	τR_1(A1)γC19-H39	980	δO2C16C10
966w	964sh	965m		966	νC11-C14	976	νC11-C14		
962sh			960sh	959	δC14N6C20	955	γC17-H38νC10-O1	962	γC17-H38
945w	951sh					946	γC23-H44γC21-H43	952	τR_1(A3)
	938w		937w	937	νC7-C12νC26-C27	941	γC23-H44	940	νC7-C12
	931sh	933w		931	$\tau_w$$CH_2$(C14)			927	γC23-H44
	927sh	920m		924	γC21-H43	922	$\tau_w$$CH_2$(C13)	921	$\tau_w$$CH_2$(C14)
910w	909sh	909m	908m	909	$\tau_w$$CH_2$(C13)	908	νC24-O2	903	βR_3(A3) τR_3(A5)
892sh	899w	891sh	902sh	904	νC10-O1	896	$\tau_w$$CH_2$(C14)	896	$\tau_w$$CH_2$(C13)
887w	886w	871m	871m	879	νC26-O3	885	τR_1(A3) βR_1(A5)	878	νC26-O3
871w		871m	871m	867	τR_1(A3)νC26-O3	866	βR_1(A5)	865	νC26-O3δC22O3C26
	860w					859	νC26-O3δC22O3C26		
838w	832sh	833m	830w	854	νC9-C13	851	νN6-C14	862	νC10-O1
822sh	815w	814m	817w	826	νC10-C16	827	νC10-C16	827	νC10-C16
819w	805sh	796sh	796w	810	γC19-H39	809	γC21-H43	807	γC21-H43
776w	771sh	780m	774w	782	$\tau_w$$CH_2$(C11)	774	τR_1(A1)	777	τR_1(A1)
766w	763sh	767m		769	βR_2(A2)			767	βR_2(A2)$\tau_w$$CH_2$(C11)
758vw	757m		760sh	756	βR_1(A4)	761	$\tau_w$$CH_2$(C11)	760	νN6-C9
750vw	750sh	742w	748sh	740	τR_2(A3) τR_1(A4)	746	βR_2(A2)	744	τR_2(A3)τR_1(A3)
728w	727sh	723w	728w	720	τR_1(A4)	730	τR_1(A4)	726	τR_1(A4)τR_2(A2)
716vw	718sh			716	τR_1(A4)	711	νN6-C9	715	τR_2(A3) τR_1(A4)
690vw	697vw		690w			707	τR_2(A3) τR_1(A4)		
680w	680sh	688w		680	γC17-H38			681	γC19-H39βR_2(A4)
661w	672w	659w				678	βR_2(A4)		
	652w	649w		651	νC24-C25	648	δCOO(C24)	650	δCOO(C24)
			634sh	638	βR_3(A3)	638	βR_3(A3)	640	βR_3(A3)τR_1(A1)
	616vs	620w	613vs	621	τR_1(A4)βR_3(A3)	620	τR_1(A4) βR_3(A3)	623	τR_1(A4)βR_3(A3)
	607sh		604sh	605	τR_1(A1)	604	τR_1(A1)	605	τR_1(A1)
	592sh	596w		601	γCOO(C24)	597	γCOO(C24)	601	γCOO(C24)
	578sh	584w		592	γCOO(C26)	591	γCOO(C24) γCOO(C26)	591	γCOO(C26)
	571m	571w	578w	572	γC22-O3	574	τR_2(A4) γC22-O3	576	γC22-O3
				564	τR_2(A3) τR_1(A3)	563	τR_2(A3)τR_1(A3)	566	τR_2(A3)τR_1(A3)
	549sh	556w	555w	557	τR_3(A4) τR_2(A2)	556	τR_2(A3) τR_3(A4)	559	τR_3(A4) γCOO(C26)

544sh	543sh	540sh	544	τR_2(A4)	535	τR_3(A4)	540	τR_3(A4)τR_2(A4)
524m	522w	528sh	522	βR_2(A4)	518	βR_1(A5)	520	βR_1(A5)
	513sh	518m			507	δC9N6C20	516	δC9N6C20
495sh			498	βR_3(A4)				
485m	493w	483w	490	βR_3(A4)	496	βR_3(A4) ρCOO(C26)	496	βR_3(A4)ρCOO(C26)
	474sh		477	βR_2(A5) ρCOO(C24)	475	βR_2(A5)βR_2(A1)	479	βR_2(A5)βR_2(A1)
460w	466w	456w	453	βR_3(A1)	444	βR_3(A1)	451	βR_3(A1)
449sh	444w	435m	439	βR_3(A3)	436	βR_3(A3)	441	βR_3(A3)
431m	420w	410w	406	βR_3(A5)	407	ρCOO(C24)	417	τR_1(A1) ρCOO(C24)
401w	413sh	394w	392	βR_2(A3)	391	βR_3(A5)βR_2(A3)	401	βR_3(A5)βR_2(A3)
364sh		365w	357	τR_2(A3)	356	τR_2(A3)τR_1(A3)	360	τR_1(A3)τR_2(A3)
342w		342m	342	βN6-C20 ρCOO(C26)	340	δC14N6C20	350	δC14N6C20
324w		334sh	336	τR_1(A3) τR_2(A3)	330	τR_1(A3) βR_2(A5)	336	τR_1(A3)τR_2(A3)
315sh		318w	320	τR_1(A1) τR_3(A1)	326	τR_1(A1) τR_3(A1)	324	τR_3(A1) δO2C16C19
305w		303sh	301	τR_1(A5)	310	τR_1(A3) τR_1(A1)	313	τR_1(A3) τR_1(A1)
283w		280sh	285	τR_3(A5) τR_2(A5)	283	τR_3(A5)τR_2(A5)	287	τR_2(A5)
276sh		272m	275	βC22-O3	271	βC22-O3	277	βC22-O3
261sh		264sh	259	τR_3(A5)	260	τR_1(A3) τR_3(A3)	265	τR_3(A3)
254m		249m			256	τR_1(A5)	257	τR_3(A5)τR_1(A5)
237m		235m	241	τR_3(A3) γC22-O3				
227sh		223sh	219	$\tau_w CH_3$(C20)τR_2(A5)			224	νH51-Cl52
			214	τR_1(A3) τR_3(A5)	216	δO2C16C10	207	δC16O2C24
200sh		204sh	203	τR_1(A3) βR_3(A3)	204	δC16O2C24	204	νH51-Cl52τR_1(A3)
196sh		194w			194	$\tau_w CH_3$(C20)	184	$\tau_w CH_3$(C20)
166s		170s	165	τR_1(A3)	164	τR_1(A3)	162	τR_1(A3)
158sh		161sh	158	δC16O2C24	156	τR_3(A5)	155	τR_3(A5)τR_1(A3)
140s		142w	133	τR_1(A2) δC22O3C26	128	τR_1(A2)	137	τR_1(A2)
116s		114sh	109	τR_2(A3) τR_3(A5)	109	τR_2(A3) τR_2(A5)	113	τR_2(A3)
100s		107vs	100	$\tau_w CH_3$(C25)			99	$\tau_w CH_3$(C25)
92sh		91sh			94	$\tau_w CH_3$(C25)	90	$\tau_w CH_3$(C27)
87sh		84sh	84	τR_1(A3) τR_3(A3)	86	$\tau_w CH_3$(C27)	85	τR_1(A3) τR_3(A3)
			83	τR_1(A3) τR_2(A3)	83	τR_3(A3)		
			74	τO2-C24	75	τO2-C24δO2C16C19	74	τO2-C24
					62	$\tau_w CH_3$(C27) τO3-C22	63	$\tau_w CH_3$(C27)τR_1(A1)
			60	$\tau_w CH_3$(C27)			60	τR_1(A1)τR_1(A3)
			50	τO3-C2	53	τO3-C2	52	τO3-C2
							44	τO3-C2τR_1(A3)
			38	τO3-C22	37	τO3-C22	35	τ_wCOO(C24)
			29	τ_wCOO(C24)	33	τ_wCOO(C24)	31	τO3-C22
			19	τR_2(A1)	16	τR_2(A1)	16	τR_2(A1)

Abbreviations: br, broad; ν, stretching; β, deformation in the plane; γ, deformation out of plane; wag, wagging; τ , torsion; β_R, deformation ring τ_R, torsion ring; ρ, rocking; τw, twisting; δ, deformation; a, antisymmetric; s, symmetric; (A_1), Ring1; (A_2), Ring2; (A_3), Ring3; (A_4), Ring4; (A_5), Ring5.

[a]This work, [b]From scaled quantum mechanics force field; [c]From Ref [18]; [d]From Ref [18]

Bands Assignments

3500-2000 cm^{-1} region. In this region are expected the N-H stretching modes only for the cationic heroin species, the aromatic and aliphatic C-H stretching modes and the antisymmetric and symmetric stretching modes of CH_2 and CH_3 groups for the three species. In clonidine hydrochloride the N-H stretching modes for cationic and hydrochloride forms were assigned at 3427 and 1711 cm^{-1} [48], in tropane alkaloid at 3419 cm^{-1} and 1626 cm^{-1} [12], in cocaine are assigned at 2982/2981 and 2545 cm^{-1} [13] while in morphine at 3356, and 1855 cm^{-1} [11]. In heroin, these modes are assigned to 3483 and 1674 cm^{-1}. In heroin species, the aromatic C-H stretching modes are assigned at higher wavenumbers than the aliphatic ones, as reported in morphine [11].

In the three heroin species, the antisymmetric and symmetric CH_3 modes are predicted by SQM calculations between 3077 and 2819 cm^{-1} and, for this reason, they are assigned to the IR and Raman bands located between 3052 and 2808 cm^{-1}, as in morphine (3206/2865 cm^{-1}), cocaine (3056/2845 cm^{-1}) and tropane alkaloids (3098/2966 cm^{-1}) [11-13]. On the other hand, in cocaine, the antisymmetric and symmetric CH_2 modes are predicted at 3009/2938 cm^{-1} [11], in tropane species at 3024/2911 cm^{-1} [30] while in morphine at 3036/2821 cm^{-1}. Hence, the bands between 3033 and 2906 cm^{-1} are easily assigned to these modes of heroin species, as predicted by calculations. Here, the intense IR band observed in the spectrum of free base at 2794 cm^{-1} and at 2455 cm^{-1} with medium intensity in the Raman spectrum of the hydrochloride form could be attributed to dimeric species not considered here. Obviously, the symmetrical modes are associated to the most intense Raman bands.

2000-1000 cm^{-1} region. Here, the C=O, C=C and C-O stretching modes, the N-H stretching mode for the hydrochloride species, antisymmetric and symmetric CH_3 deformation modes, CH_2 deformation modes, C-H, CH_2 and CH_3 rocking modes and CH_2 wagging modes are predicted by B3LYP/6-31G* calculations of those three heroin species. The assignments of all these modes can be seen in Table 9. The strong IR bands at 1754 and 1733 cm^{-1} in the spectrum of hydrochloride form are assigned respectively to the two C26=O5 and C24=O4 stretching modes while the intense Raman band at 1674 cm^{-1} is assigned to the N-H stretching mode for the hydrochloride species, as was explained in the above section. The intense Raman band at 1645 cm^{-1} is simultaneously assigned to two C17=C19 and C12=C18 stretching modes predicted in the same regions for the three heroin species. Note that the strong IR and Raman bands at 1439 and 1435 cm^{-1}, respectively can be indistinctly assigned

to C8-O1 stretching modes and to CH_3 and CH_2 deformation modes because the calculations have predicted some of these modes in this region. In this region, results few commons were obtained, for instance, the two deformation modes of acetyl group, identified in the three heroin species as δCOO(C26) and (δCOO(C24), are predicted by SQM calculations between 1240 and 1007 cm^{-1} when normally these modes are assigned between 800 and 600 cm^{-1} [28,49-51], including in cocaine [13]. Evidently, these groups in the three heroin species are strongly influenced by the different five fused rings, especially the δCOO(C26) group linked to aromatic R4 ring in the three species. Apparently, in the heroin species the two acetyl groups do not present movements free as in the cocaine species and, for these reasons, in the following section, the force constants were also calculated in order to explain these differences. Other unusual obtained result was observed in the expected deformations ring modes of R1, R3, R4 and R5 rings because these modes are normally predicted and assigned below 1000 cm^{-1} [25,27,29, 31,32] and, here, in the three heroin species some of these modes (βR_1 and βR_3) are predicted from 1228 cm^{-1}, as observed in Table 9.

2000-1000 cm^{-1} region. In this region are expected the vibration modes of acetyl groups (wagging, γCOO; rocking, ρCOO and twisting, τ_wCOO modes), deformation (βR_1, βR_2 and βR_3) and torsion (τR_1, τR_2 and τR_3) rings of five rings and, other skeletal vibrations (C-C and C-O stretching modes, OCC, CNC, COC, OCO deformations and, CH_3 and CH_2 twisting modes. Here, it is necessary to clarify the only for the R2 ring of five members is expected two deformations and two torsions rings. All these modes were assigned in accordance to the SQM calculations and, as detailed in Table 9.

Here, the identifications of N6-CH_3 stretching modes (N6-C20) in the three heroin species are of interest because they play a very important role in the pharmacological and medicinal properties of all tropane alkaloids and, for these reasons, they are here analyzed. In the three tropane species these modes were assigned at 1128, 1086 and 1031 cm^{-1}, in the cocaine species at 1113, 1058 and 1052 cm^{-1} and, in the free base of morphine at 1160 cm^{-1}, in the cationic form at 984 cm^{-1} and in the hydrochloride form of this species at 1047 cm^{-1}. Here, in the free base, cationic and hydrochloride forms of heroin that mode is assigned to the bands at 1094, 989 and 1017 cm^{-1}, respectively, in accordance to the calculations.

Force constants

For the three heroin species in both media were computed the harmonic force constants from their corresponding harmonic force fields obtained at B3LYP/6-31G* level of theory by using the SQMFF procedure [16] and the Molvib program [17]. The scaled internal force constants are presented in **Table 10** compared with those reported for morphine, cocaine and tropane alkaloids in both media [11-13]. Analyzing first the force constants for the three heroin species, it is observed that the presence of Cl atom in the hydrochloride species drastically reduce the force constant *f(νN-H)* values in both media, observing for the hydrochloride form a low value in gas phase. When this constant is compared with the other alkaloids cocaine present the higher values in both media. Comparing then the *f(νN-CH$_3$)* force constants, the cationic forms of all alkaloids in both media have the lower values than the other ones probably due to the presence of N-H groups positively charged and, hence, the values slightly increase in solution.

Table 10. Scaled internal force constants for the free base, cationic and hydrochloride heroin species compared with the corresponding to morphine, cocaine and tropane species in gas and aqueous solution phases.

B3LYP/6-31G*						
Heroin[a]						
Force constant	Free base		Cationic		Hydrochloride	
	Gas	PCM	Gas	PCM	Gas	PCM
f(νN-H)			5.93	5.93	2.67	4.54
f(νN-CH$_3$)	4.83	4.67	4.04	4.09	4.38	4.26
f(νC=O)	12.50	11.62	12.67	11.62	12.55	11.65
f(νC-O)	5.07	5.06	4.39	5.04	5.05	5.05
f(νC-O)$_R$	5.23	4.92	5.30	4.98	5.27	4.91
f(νC-N)	4.88	4.77	3.76	4.01	4.30	4.17
f(νCH$_2$)	4.69	4.73	4.84	4.89	4.83	4.89
f(νCH$_3$)	4.88	4.91	5.01	4.98	4.98	5.02
f(νC-H)$_R$	5.14	5.16	5.18	5.17	5.15	5.18
f(νC-H)	4.72	4.81	4.71	4.84	4.77	4.85
f(νC-C)	4.18	4.33	4.24	4.33	4.19	4.33
f(δCOO)	1.36	1.39	1.38	1.37	1.37	1.37
f(δCH$_2$)	0.74	0.72	0.73	0.72	0.73	0.72

f(δCH$_3$)	0.57	0.56	0.55	0.56	0.55	0.54

Morphine[b]

Force constant	Free base		Cationic		Hydrochloride	
	Gas	PCM	Gas	PCM	Gas	PCM
f(νO-H)	7.12	7.13	7.21	7.13	7.13	7.05
f(νN-H)			5.93	5.98	2.73	4.61
f(νN-CH$_3$)	4.83	4.69	4.05	4.15	4.37	4.25
f(νC-N)	4.74	4.59	3.67	3.91	4.20	4.03
f(νCH$_2$)	4.69	4.72	4.85	4.90	4.82	4.89
f(νCH$_3$)	4.70	4.76	5.08	5.12	5.01	5.09
f(νC-H)	4.65	4.71	4.62	4.77	4.72	4.79
f(νC-C)	5.74	5.73	6.04	5.77	5.79	5.78
f(δCH$_2$)	0.74	0.73	0.73	0.72	0.73	0.72
f(δCH$_3$)	0.58	0.57	0.56	0.56	0.56	0.56

Cocaine[c]

Force constant	Free base		Cationic		Hydrochloride	
	Gas	PCM	Gas	PCM	Gas	PCM
f(νN-H)			4.91	5.55	3.23	4.79
f(νN-CH$_3$)	4.69	4.52	4.17	4.23	4.31	4.17
f(νC-N)	4.20	4.01	3.41	3.51	3.71	3.54
f(νCH$_2$)	4.85	4.87	4.91	4.93	4.88	4.93
f(νCH$_3$)	4.86	4.92	5.07	5.09	5.04	5.08
f(νC-H)	4.86	4.91	4.93	5.02	4.91	4.98
f(νC-C)	3.94	3.98	4.06	4.09	4.08	4.11
f(δCOO)	1.46	1.43	1.52	1.45	1.49	1.45
f(δCH$_2$)	0.74	0.72	0.75	0.73	0.75	0.73
f(δCH$_3$)	0.58	0.56	0.57	0.56	0.57	0.56

Tropane[d]

Force constant	Free base		Cationic		Hydrochloride	
	Gas	PCM	Gas	PCM	Gas	PCM
f(νN-H)			5.97	5.98	2.70	4.69
f(νN-CH$_3$)	4.69	4.52	4.09	4.21	4.42	4.26
f(νC-N)	4.16	3.97	3.11	3.35	3.73	3.48
f(νCH$_2$)	4.78	4.78	4.88	4.88	4.85	4.87
f(νCH$_3$)	4.72	4.79	5.10	5.13	5.03	5.11
f(νC-H)	4.78	4.82	4.92	4.99	4.90	4.96
f(νC-C)	4.05	4.06	4.17	4.21	4.16	4.20
f(δCH$_2$)	0.74	0.72	0.75	0.72	0.74	0.73

$f(\delta CH_3)$	0.58	0.57	0.56	0.56	0.56	0.56

Units are mdyn Å^{-1} for stretching and mdyn Å rad^{-2} for angle deformations

[a]This work; [b]From Ref [11]; [c]From Ref [13]; [d]From Ref [12]

The $f(\nu C{=}O)$ constants values corresponding to the acetyl groups change in solution, as expected because these groups are probably hydrated in solution while the $f(\nu C\text{-}O)_R$ constants corresponding to the C-O bonds of R2 rings practically do not change in the three species but in solution slight decreasing are observed in the different forms. The other $f(\nu C\text{-}O)$ constants practically present the same values. Here, the assignments of deformation modes of acetyl groups (δCOO) to higher wavenumbers than those reported values for other compounds with similar groups [28,49-51] could be justified by the higher values observed in the $f(\delta COO)$ force constants, for example, in relation to the cocaine value. The other force constants observed in Table 10 present practically the same behaviors in both media.

CONCLUSIONS

Here, the structures of the free base, cationic and hydrochloride heroin species were theoretically determined in gas phase and in aqueous solution employing the hybrid B3LYP/6-31G* method. The solvent effects were studied by using the SCRF and PCM methods while the solvation energies were predicted with the solvation model. The three species in both media were optimized with N-CH_3 groups in equatorial positions which apparently favour the volume expansions in solution. The three Heroin species presents the higher solvation energy values, as compared with the corresponding to morphine and cocaine. The charges studies and the MEP mapped surfaces suggest clear electrophilic sites on the N-H group of the cationic species while the hydrochloride species shows nucleophilic regions around the Cl atoms but less weak sites on the C=O groups. The low BO values for the Cl atoms in the hydrochloride species in both media reveal the ionic characteristics of their halogen H---Cl bonds. The NBO and AIM studies support the high stabilities of those three heroin species against to the corresponding to morphine and cocaine. Here, the presence of other groups linked to tropane ring increase significantly the reactivity of alkaloid, specifically of its cationic and hydrochloride forms. The predicted higher global electrophilicity index (ω) for hydrochloride form of cocaine and the low global nucleophilicity index (E) values in heroin and morphine could probably explain the different

behaviors of these species in both media. In this work, the broadly known potential pharmacological properties for the three heroin species were explained easily with the rule of five states suggested by Lipinski's and Veber. The harmonic force fields and the complete vibrational assignments of the 144, 147 and 150 normal vibration modes expected respectively for the free base, cationic and hydrochloride heroin species were here reported for first time by using the SQMFF methodology.

ACKNOWLEDGEMENTS.

This work was supported with grants from CIUNT Project Nº 51/D608 (Consejo de Investigaciones, Universidad Nacional de Tucumán). The author would like to thank Prof. Tom Sundius for his permission to use MOLVIB.

REFERENCES

[1] Busse GD, Drugs, The Straight Facts, Morphine, Consulting Editor David J. Triggle, Chelsea House Publishers, New Cork (2006).
[2] Rinner U, Hudlicky T, Synthesis of Morphine Alkaloids and Derivatives, Top Curr Chem 2012; 309: 33–66.
[3] Pandey AK, Dwivedi A, Siddiqui SA, Misra N, Vibrational Spectra of Two Narcotics. A DFT Study, Chinese J. of Physics 2013; 51(3): 473-499.
[4] Sweta VR, Lakshmi, T. Pharmacological profile of tropane alkaloids, Journal of Chemical and Pharmaceutical Research, 2015; 7(5): 117-119.
[5] Penido, CA, Pacheco MT, Zângaro RA, Silveira L Jr, Identification of different forms of cocaine and substances used in adulteration using near-infrared Raman spectroscopy and infrared absorption spectroscopy, J Forensic Sci. 2015; 60(1): 171-178.
[6] Singh Bumbrah G, Sharma RM, Raman spectroscopy-Basic principle, instrumentation and selected applications for the characterization of drugs of abuse, Egyptian J. Forensic Sci. 2016; 6: 209-215.
[7] Guha, P.; Harraz, M.M.; Snyder, S.H., Cocaine elicits autophagic cytotoxicity via a nitric oxide-GAPDH signaling cascade, PNAS, 2016; 113(5): 1417-1422.
[8] Fernandes de Oliveira Penido CA, Tavares Pacheco MT, Lednev IK, Silveira Jr L, Raman spectroscopy in forensic analysis: identification of cocaine and other illegal drugs of abuse, J. Raman Spectrosc. 2016; 47: 28–38.
[9] Moros J, Galipienso N, Vilches R, Garrigues S, de la Guardia M, Nondestructive Direct Determination of Heroin in Seized Illicit Street Drugs by Diffuse Reflectance near-Infrared Spectroscopy, Anal. Chem. 2008; 80: 7257–7265.
[10] Hodges CM, Hendra PJ, Willis HA, Farley T, Fourier transform Raman spectroscopy of illicit drugs, J Raman Spectroscopy, 1989; 20(11): 745-749.
[11] Brandán SA, Why morphine is a molecule chemically powerful. Their comparison with cocaine, Indian Journal of Applied Research, 2017; 7(7): 511-528.
[12] Rudyk RA, Brandán SA, Force field, internal coordinates and vibrational study of alkaloid tropane hydrochloride by using their infrared spectrum and DFT calculations, Paripex A Indian Journal of Research, 2017; 6(8): 616-623.
[13] Romani D, Brandán SA, Vibrational analyses of alkaloid cocaine as free base, cationic and hydrochloride species based on their internal coordinates and force fields, Paripex A Indian Journal of Research, 2017; 6(9): 587-602.

[14] Horváth E., Mink J., Kristóf J. Surface-enhanced Raman Spectroscopy as a Technique for Drug Analysis. In: Mink J., Keresztury G., Kellner R. (eds) Progress in Fourier Transform Spectroscopy. Mikrochimica Acta Supplement, vol 14. Springer, Vienna (1997).
[15] Pulay, P.; Fogarasi, G.; Pongor, *G.;* Boggs, J. E.; Vargha, A. Combination of theoretical ab initio and experimental information to obtain reliable harmonic force constants. Scaled quantum mechanical (QM) force fields for glyoxal, acrolein, butadiene, formaldehyde, and ethylene, J. Am. Chem. Soc. 1983; 105: 7073.
[16] Rauhut G, Pulay P, Transferable Scaling Factors for Density Functional Derived Vibrational Force Fields, J. Phys. Chem. 1995; 99: 3093-3100. b) *Correction:* G. Rauhut, P. Pulay, J. Phys. Chem. 1995; 99: 14572.
[17] Sundius T. Scaling of ab-initio force fields by MOLVIB. Vib. Spectrosc. 2002; 29:89-95.
[18] Available from: file:///C:/Users/Usuario/Downloads/HEROIN.pdf.
[19] Canfield D, Barrick J, Giessen BC, Structure of Diacetylmorphine (Heroin) Acta Cryst. 1979; B35: 2806-2809.
[20] Deschamps JR, George C, Flippen-Anderson JL, A Diacetylmorphine Polymorph Acta Cryst. 1996; C52: 698-700.
[21] Becke AD. Density functional thermochemistry. III. The role of exact exchange. J. Chem. Phys. 1993; 98:5648-5652.
[22] Lee C, Yang W, Parr R.G. Development of the Colle-Salvetti correlation-energy formula into a functional of the electron density. Phys. Rev. 1988; B37: 785-789.
[23] Parr RG, Pearson RG. Absolute Hardness: companion parameter to absolute electronegativity. J. Am. Chem. Soc. 1983; 105:7512-7516.
[24] Brédas J-L. Mind the gap!. Materials Horizons 2014; 1:17–19.
[25] Romani D, Márquez MJ, Márquez MB, Brandán SA. Structural, topological and vibrational properties of an isothiazole derivatives series with antiviral activities. J. Mol. Struct. 2015; 1100:279-289.
[26] Romani D, Tsuchiya S, Yotsu-Yamashita M, Brandán SA, Spectroscopic and structural investigation on intermediates species structurally associated to the tricyclic bisguanidine compound and to the toxic agent, saxitoxin, J. Mol. Struct. 2016; 1119: 25-38.
[27] Chain F, Iramain MA, Grau A, Catalán CAN, Brandán SA, Evaluation of the structural, electronic, topological and vibrational properties of *N*-(3,4-dimethoxybenzyl)-hexadecanamide isolated from Maca (*Lepidium meyenii*) using different spectroscopic techniques, J. Mol. Struct. 2016; 1119: 25-38.
[28] Issaoui N, Ghalla H, Brandán SA, Bardak F, Flakus HT, Atac A, Oujia B, Experimental FTIR and FT-Raman and theoretical studies on the molecular structures of monomer and dimer of 3-thiopheneacrylic acid, J. Mol. Struct. 2017; 1135: 209-221.
[29] Chain FE, Ladetto MF, Grau A, Catalán CAN, Brandán SA, Structural, electronic, topological and vibrational properties of a series of N-benzylamides derived from Maca (*Lepidium meyenii*) combining spectroscopic studies with ONION calculations, J. Mol. Struct. 2016; 1105: 403-414.
[30] Minteguiaga M, Dellacassa E, Iramain MA, Catalán CAN, Brandán SA, Synthesis, Spectroscopic characterization and structural study of carquejiphenol, a 2-Isopropenyl-3-methylphenol derivative with potential medicinal uses, J. Mol. Struct. 2018; 1165: 332-343.
[31] Iramain MA, Davies L, Brandán SA, FTIR, FT-Raman and UV-visible spectra of Potassium 3-furoyltrifluoroborate salt, J. Mol. Struct. 2018; 1158: 245-254.
[32] Iramain MA, Davies L, Brandán SA, Evaluating structures, properties and vibrational and electronic spectra of the Potassium 2-isonicotinoyl trifluoroborate salt, J. Mol. Struct. 2018; 1163: 41-53.
[33] Edrik J, Bautista K, Merhi B, Gregory O, Hu S, Henriksen K, Gohh R, Heroin crystal nephropathy, Clinical Kidney Journal, 2015; 8(3): 339–342.
[34] Nielsen AB, Holder AJ. 2008. *Gauss View* 5.0, User's Reference, GAUSSIAN Inc., Pittsburgh, PA.
[35] Gaussian 09, Revision A.02, Frisch, M. J.; Trucks, G. W.; Schlegel, H. B.; Scuseria, G. E.; Robb, M. A.; Cheeseman, J. R.; Scalmani, G.; Barone, V.; Mennucci, B.; Petersson, G. A.; Nakatsuji, H.; Caricato, M.; Li, X.; Hratchian, H. P.; Izmaylov, A. F.; Bloino, J.; Zheng, G.; Sonnenberg, J. L.; Hada, M.; Ehara, M.; Toyota, K.; Fukuda, R.; Hasegawa, J.; Ishida, M.; Nakajima, T.; Honda, Y.; Kitao, O.; Nakai, H.; Vreven, T.; Montgomery, J. A., Jr.; Peralta, J. E.; Ogliaro, F.; Bearpark, M.; Heyd, J. J.; Brothers, E.; Kudin, K. N.; Staroverov, V. N.; Kobayashi, R.; Normand, J.; Raghavachari, K.; Rendell, A.; Burant, J. C.; Iyengar, S. S.; Tomasi, J.; Cossi, M.; Rega, N.; Millam, J. M.; Klene, M.; Knox, J. E.; Cross, J. B.; Bakken, V.; Adamo, C.; Jaramillo, J.; Gomperts,

R.; Stratmann, R. E.; Yazyev, O.; Austin, A. J.; Cammi, R.; Pomelli, C.; Ochterski, J. W.; Martin, R. L.; Morokuma, K.; Zakrzewski, V. G.; Voth, G. A.; Salvador, P.; Dannenberg, J. J.; Dapprich, S.; Daniels, A. D.; Farkas, Ö.; Foresman, J. B.; Ortiz, J. V.; Cioslowski, J.; Fox, D. J. Gaussian, Inc., Wallingford CT, 2009.

[36] Miertus S, Scrocco E, Tomasi J. Electrostatic interaction of a solute with a continuum. Chem**.** Phys**.** 1981; 55:117–129.

[37] Tomasi J, Persico J. Molecular Interactions in Solution: An Overview of Methods Based on Continous Distributions of the Solvent. Chem. Rev. 1994; 94:2027-2094.

[38] Marenich AV, Cramer CJ, Truhlar D.G. Universal solvation model based on solute electron density and a continuum model of the solvent defined by the bulk dielectric constant and atomic surface tensions. J. Phys. Chem. 2009; B113:6378-6396.

[39] Ugliengo P. MOLDRAW Program, University of Torino, Dipartimento Chimica IFM, Torino, Italy, 1998.

[40] Glendening ED, Badenhoop JK, Reed AD, Carpenter JE, Weinhold F. 1996. NBO 3.1; Theoretical Chemistry Institute, University of Wisconsin; Madison.

[41] Besler BH, Merz Jr KM, Kollman PA, Atomic charges derived from demiempirical methods, J. Comp. Chem. 1990; 11: 431-439.

[42] Biegler-Köning F, Schönbohm J, Bayles DJ. AIM2000; a program to analyze and visualize atoms in molecules. Comput. Chem. 2001; 22:545-559.

[43] Bader RFW. Atoms in Molecules. A Quantum Theory, Oxford University Press, Oxford, ISBN: 0198558651; 1990.

[44] Lipinski CA, Lombardo F, Dominy BW, Feeney PJ, Experimental and computational approaches to estimate solubility and permeability in drug discovery and development settings, Adv Drug Deliv Rev 2001; 46(1-3): 3-26.

[45] Veber DF, Johnson SR, Cheng HY, Smith BR, Ward KW, Kopple KD, Molecular properties that influence the oral bioavailability of drug candidates, J Med Chem. 2002; 45(12): 2615-23.

[46] Keresztury G, Holly S, Besenyei G, Varga J, Wang AY, Durig JR, Vibrational spectra of monothiocarbamates-II. IR and Raman spectra, vibrational assignment, conformational analysis and ab initio calculations of **S**-methyl-N,N-dimethylthiocarbamate, Spectrochim. Acta, 1993; 49A: 2007-2026.

[47] Michalska D, Wysokinski R, The prediction of Raman spectra of platinum(II) anticancer drugs by density functional theory, Chem. Phys Letters, 2005; 403: 211-217.

[48] Romano E, Davies L, Brandán SA, Structural properties and FTIR-Raman spectra of the anti-hypertensive clonidine hydrochloride agent and their dimeric species, J. Mol. Struct. 2017; 1133: 226-235.

[49] Chain F, Romano E, Leyton P, Paipa C, Catalan CAN, Fortuna MA, Brandan SA, An experimental study of the structural and vibrational properties of sesquiterpene lactone cnicin using FT-IR, FT-Raman, UV–visible and NMR spectroscopies, J. Mol Struct. 2014; 1065-1066: 160–169.

[50] Guzzetti KA, Brizuela AB, Romano E, Brandán SA, Structural and vibrational study on zwitterions of L-threonine in aqueous phase using the FT-Raman and SCRF calculations J. Mol. Struct. 2013; 1045: 171–179.

[51] Romano E, Castillo MV, Pergomet J, Zinczuk J, Brandán SA, Synthesis and structural and vibrational analysis of (5,7-dichloro-quinolin-8-yloxy) acetic acid J. Mol. Struct. 2012; 1018: 149–155.